

**AD-A249 637**



**USAARL Report No. 92-13**

**DTIC**

**ELECTE**

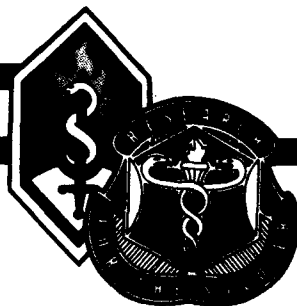
**APR 28 1992**

**S**

**C**

**D**

**①**



**Field-of-View Evaluation  
of the Preplanned Product Improvement  
Visual Correction  
of the M40 Protective Mask**

**By**

**John C. Kotulak**

**and**

**John K. Crosley**

**Sensory Research Division**

**February 1992**

**92-10674**



**02 4 24 111**

**Approved for public release; distribution unlimited.**

**United States Army Aeromedical Research Laboratory  
Fort Rucker, Alabama 36362-5292**

## Notice

### Qualified requesters

Qualified requesters may obtain copies from the Defense Technical Information Center (DTIC), Cameron Station, Alexandria, Virginia 22314. Orders will be expedited if placed through the librarian or other person designated to request documents from DTIC.

### Change of address

Organizations receiving reports from the U.S. Army Aeromedical Research Laboratory on automatic mailing lists should confirm correct address when corresponding about laboratory reports.

### Disposition

Destroy this report when it is no longer needed. Do not return to the originator.

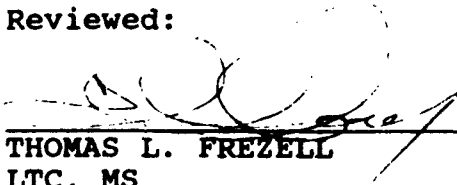
### Disclaimer

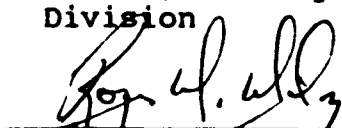
The views, opinions, and/or findings contained in this report are those of the authors and should not be construed as an official Department of the Army position, policy, or decision, unless so designated by other official documentation. Citation of trade names in this report does not constitute an official Department of the Army endorsement or approval of the use of such commercial items.

### Human use

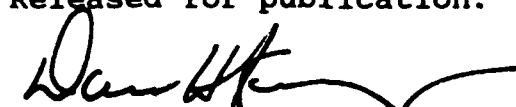
Human subjects participated in these studies after giving their free and informed voluntary consent. Investigators adhered to AR 70-25 and USAMRDC Reg 70-25 on Use of Volunteers in Research.

Reviewed:

  
THOMAS L. FREZELL  
LTC, MS  
Director, Sensory Research  
Division

  
ROGER W. WILEY, O.D., Ph.D.  
Chairman, Scientific  
Review Committee

Released for publication:

  
DAVID H. KARNEY  
Colonel, MC, SFS  
Commanding

Unclassified

SECURITY CLASSIFICATION OF THIS PAGE

REPORT DOCUMENTATION PAGE				Form Approved OMB No. 0704-0188	
1a. REPORT SECURITY CLASSIFICATION Unclassified			1b. RESTRICTIVE MARKINGS		
2a. SECURITY CLASSIFICATION AUTHORITY			3. DISTRIBUTION / AVAILABILITY OF REPORT Approved for public release; distribution unlimited		
2b. DECLASSIFICATION / DOWNGRADING SCHEDULE					
4. PERFORMING ORGANIZATION REPORT NUMBER(S) USAARL Report No. 92-13			5. MONITORING ORGANIZATION REPORT NUMBER(S)		
6a. NAME OF PERFORMING ORGANIZATION U.S. Army Aeromedical Research Laboratory		6b. OFFICE SYMBOL (if applicable) SGRD-UAS-VS	7a. NAME OF MONITORING ORGANIZATION U.S. Army Medical Research and Development Command		
6c. ADDRESS (City, State, and ZIP Code) P.O. Box 577 Fort Rucker, AL 36362-5292			7b. ADDRESS (City, State, and ZIP Code) Fort Detrick Frederick, MD 21702-5012		
8a. NAME OF FUNDING / SPONSORING ORGANIZATION		8b. OFFICE SYMBOL (if applicable)	9. PROCUREMENT INSTRUMENT IDENTIFICATION NUMBER		
8c. ADDRESS (City, State, and ZIP Code)			10. SOURCE OF FUNDING NUMBERS		
PROGRAM ELEMENT NO. 0602787A		PROJECT NO. 3M162 787879	TASK NO. BG	WORK UNIT ACCESSION NO. 164	
11. TITLE (Include Security Classification) Field-of-View Evaluation of the Preplanned Product Improvement Visual Correction of the M40 Protective Mask					
12. PERSONAL AUTHOR(S) Kotulak, John C., and Crosley, John K.					
13a. TYPE OF REPORT Final		13b. TIME COVERED FROM _____ TO _____	14. DATE OF REPORT (Year, Month, Day) 1992 February		15. PAGE COUNT 36
16. SUPPLEMENTARY NOTATION					
17. COSATI CODES			18. SUBJECT TERMS (Continue on reverse if necessary and identify by block number)		
FIELD	GROUP	SUB-GROUP	field-of-view, protective mask, visual correction, preplanned product improvement, M40, M17, vertex distance		
20	06				
23	02				
19. ABSTRACT (Continue on reverse if necessary and identify by block number)					
<p>The purpose of this study was to evaluate the field-of-view (FOV) of a proposed preplanned product improvement (P<sup>3</sup>I) visual correction for the M40 protective mask. Two prototype mounting brackets for the P<sup>3</sup>I visual correction were used in the investigation: one with an eye well loop and the other with a Velcro<sup>TM</sup> strip. It was found that the proposed P<sup>3</sup>I visual correction provides the same FOV as its predecessor despite its larger size. The failure of the proposed P<sup>3</sup>I visual correction to provide a larger FOV was determined to be excessive vertex (eye to visual correction) distance. In addition, it was found that there was no difference between the FOVs obtained with either of the two mounting brackets. The study identified a problem of excessive vertex distance when the P<sup>3</sup>I visual correction is worn inside M40 mask sizes small and large.</p>					
20. DISTRIBUTION / AVAILABILITY OF ABSTRACT <input checked="" type="checkbox"/> UNCLASSIFIED/UNLIMITED <input type="checkbox"/> SAME AS RPT <input type="checkbox"/> DTIC USERS			21. ABSTRACT SECURITY CLASSIFICATION Unclassified		
22a. NAME OF RESPONSIBLE INDIVIDUAL Chief, Scientific Information Center			22b. TELEPHONE (Include Area Code) (205) 255-6907		22c. OFFICE SYMBOL SGRD-UAX-SI

### Acknowledgments

The authors wish to thank the following: COL Donald E. Dunphy of the Optical Fabrication Laboratory, Fitzsimons Army Medical Center, and CDR Ronald C. Nelson of the Naval Ophthalmic Support and Training Activity for providing visual corrections for the M17 and M40 protective masks respectively; LTC Luther D. Solverson of the U.S. Army Environmental Hygiene Agency for providing unpublished data on vertex distance for an earlier version of the M40 mask preplanned product improvement visual correction; SGT Marvalee P. DeCambre of this Laboratory for fitting the protective masks; Mr. William M. Fritch and Mr. William A. McCullough of the U.S. Army Chemical Research, Development, and Engineering Center for providing the M17 and M40 mask fitting sets respectively; and Mr. Simon C. Grase of this Laboratory for providing technical assistance with all phases of the study.

## Table of contents

List of figures.....	2
List of tables.....	3
Introduction.....	5
Methods.....	10
Subjects.....	10
Mask fitting.....	10
Visual corrections.....	10
FOV terminology.....	11
FOV apparatus.....	11
FOV measurement procedures.....	11
Vertex distance apparatus.....	13
Vertex distance measurement procedures.....	13
Results.....	14
Total FOV through protective masks without visual corrections.....	14
Binocular FOV through protective masks without visual corrections.....	17
Total FOV through protective masks with visual corrections.....	18
Binocular FOV through protective masks with visual corrections.....	18
Mask lens size and vertex distance.....	18
Visual correction vertex distance.....	21
Discussion.....	26
Conclusions.....	29
References.....	30

## Table of contents (continued)

### Appendixes

Appendix A - Extract from tasking document.....	33
Appendix B - Technical characteristics of M40 visual corrections.....	35

### List of figures

1. Soldier wearing M40 protective mask.....	6
2. Current visual correction for M40 protective mask.....	6
3. Preplanned product improvement visual correction for M40 protective mask.....	7
4. M40 preplanned product improvement visual correction with eye well loop mount.....	7
5. M40 preplanned product improvement visual correction with Velcro™ mount.....	8
6. Two visual corrections used in M17 protective mask.....	8
7. Field-of-view measurement apparatus.....	12
8. Vertex distance measurement apparatus.....	13
9. Total field-of-view wearing masks without visual corrections.....	15
10. Loss to total field-of-view caused by wearing protective masks without visual corrections.....	15
11. Binocular field-of-view wearing protective masks without visual corrections.....	16
12. Loss to binocular field-of-view caused by wearing masks without visual corrections.....	16
13. Total field-of-view wearing protective masks with visual corrections.....	19
14. Loss to total field-of-view caused by wearing protective masks with visual corrections.....	19
15. Binocular field-of-view wearing protective masks with visual corrections.....	20

### Table of contents (continued)

16.	Loss to binocular field-of-view caused by wearing protective masks with visual corrections.....	20
17.	Effect of mask type on mask vertex distance.....	22
18.	Effect of mask and visual correction type on visual correction vertex distance.....	22
19.	Vertex distance, M40 preplanned product improvement visual correction, all mask sizes combined.....	24
20.	Effect of M40 mask size on preplanned product improvement visual correction vertex distance.....	24
21.	Predicted versus measured fields-of-view with visual corrections.....	27
22.	Theoretical field-of-view, M40 preplanned product improvement visual correction, with and without interference by mask.....	27

### List of tables

1.	Visual corrections tested.....	9
2.	Size and curvature of mask lenses.....	10
3.	Contrast over a within factor, visual correction vertex distance as a function of visual correction type.....	23
4.	Multiple comparison tests, P <sup>3</sup> I vertex distance as a function of M40 mask size.....	25

Accession For	
NTIS GRA&I	<input checked="" type="checkbox"/>
DTIC TAB	<input type="checkbox"/>
Unannounced	<input type="checkbox"/>
Justification	
By _____	
Distribution/	
Availability Codes	
Dist	Avail and/or Special
A-1	

=====

This page intentionally left blank.

=====



## Introduction

The purpose of this study was to do a preproduction qualification test (PPQT) on a preplanned product improvement (P<sup>3</sup>I) of the M40 protective mask. Specifically, the visual field and field-of-view (FOV) of the P<sup>3</sup>I visual correction were evaluated. The authority for the PPQT is the M40 P<sup>3</sup>I Test and Evaluation Master Plan (TEMP), approved 19 December 1990. A table, which is extracted from paragraph 4b(3)(e) of the TEMP and which defines the extent of the current study, is provided as Appendix A.

The terms FOV and visual field have been used interchangeably in previous investigations of protective masks (Rash and McLean, 1983; McLean and Rash, 1984; Rash and Crosley, 1985). However, in strict usage FOV specifies an attribute of an optical instrument, while visual field specifies the analogous attribute of the human eye (Schapero, Cline, and Hofstetter, 1968). This attribute is the extent of object space visible to the observer. Therefore, in this report the term visual field refers to measurements obtained in the unmasked condition, while FOV refers to reductions in visual field brought about by the limiting apertures of the mask, visual correction, or both.

The FOV obtained with the M40 P<sup>3</sup>I visual correction was evaluated by comparing it to FOVs obtained with other mask visual corrections. Since no such data existed in the scientific literature, FOV measurements on the present M40 visual correction and two M17 protective mask visual corrections were included in this study. The FOV through the M40 P<sup>3</sup>I visual correction was evaluated with two separate mounting systems, one using an eye well loop and the other a Velcro™ strip.

The M40 and its current visual correction are pictured in Figures 1 and 2, respectively. Figure 3 shows the P<sup>3</sup>I visual correction lens carrier isolated from its mounting device, while Figures 4 and 5 show the carrier attached to the eye well loop and the Velcro™ strip mounting brackets, respectively. Figure 6 shows the two M17 visual corrections.

The technical characteristics of the current and P<sup>3</sup>I visual corrections of the M40 are described in detail in Appendix B. The most obvious difference between the two with respect to FOV is the size of the lens aperture, which is significantly larger in the P<sup>3</sup>I version (Table 1). From this, one would expect that the FOV would be proportionally greater in the P<sup>3</sup>I visual correction, but our data did not show this. To test whether this unexpected result was related to differences between the two corrections in vertex distance (distance between the anterior surface of the cornea and the posterior surface of a lens),



Figure 1. Soldier wearing M40 protective mask.

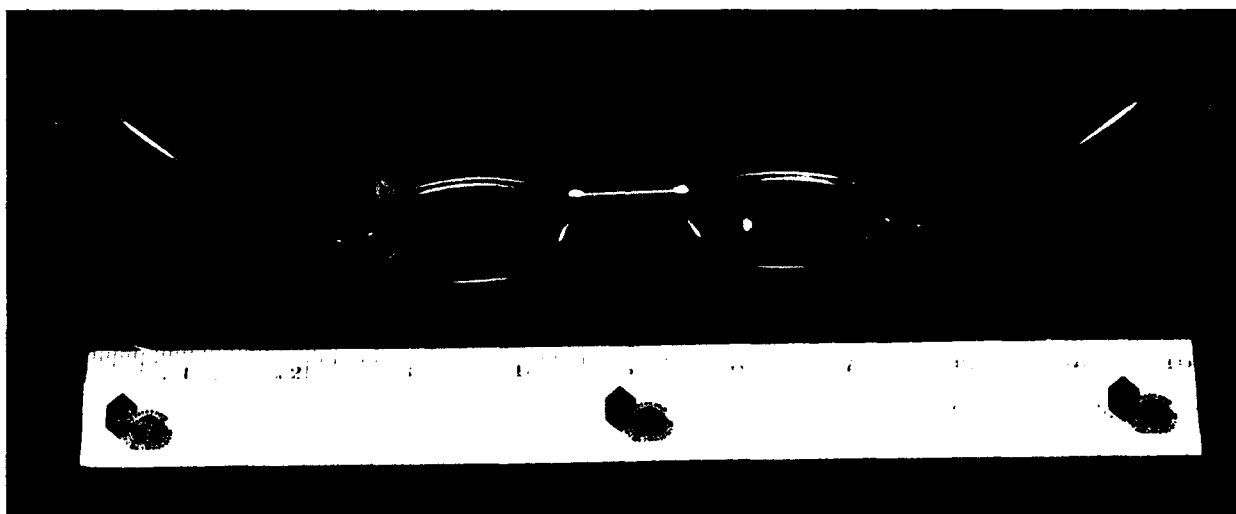


Figure 2. Current visual correction for M40 protective mask.

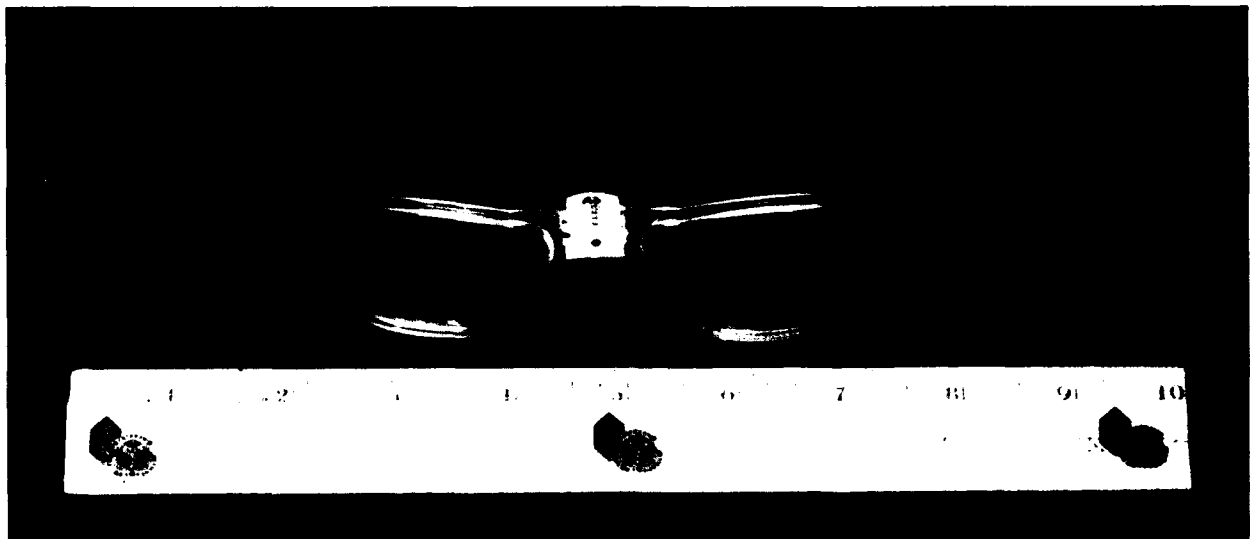


Figure 3. Preplanned product improvement visual correction for M40 protective mask.

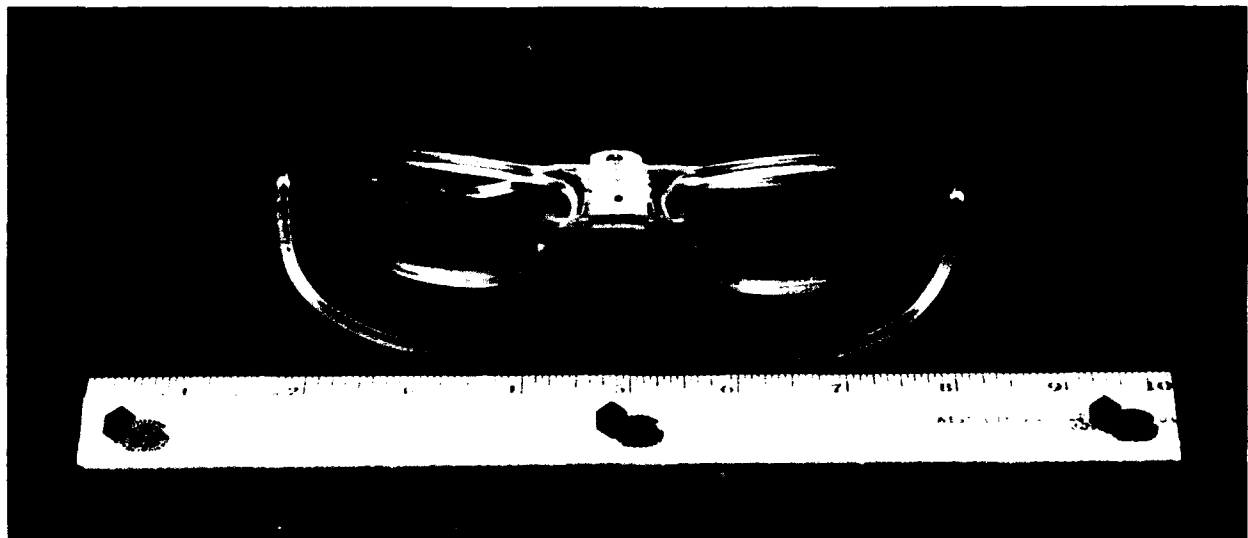


Figure 4. M40 preplanned product improvement visual correction with eye well loop mount.

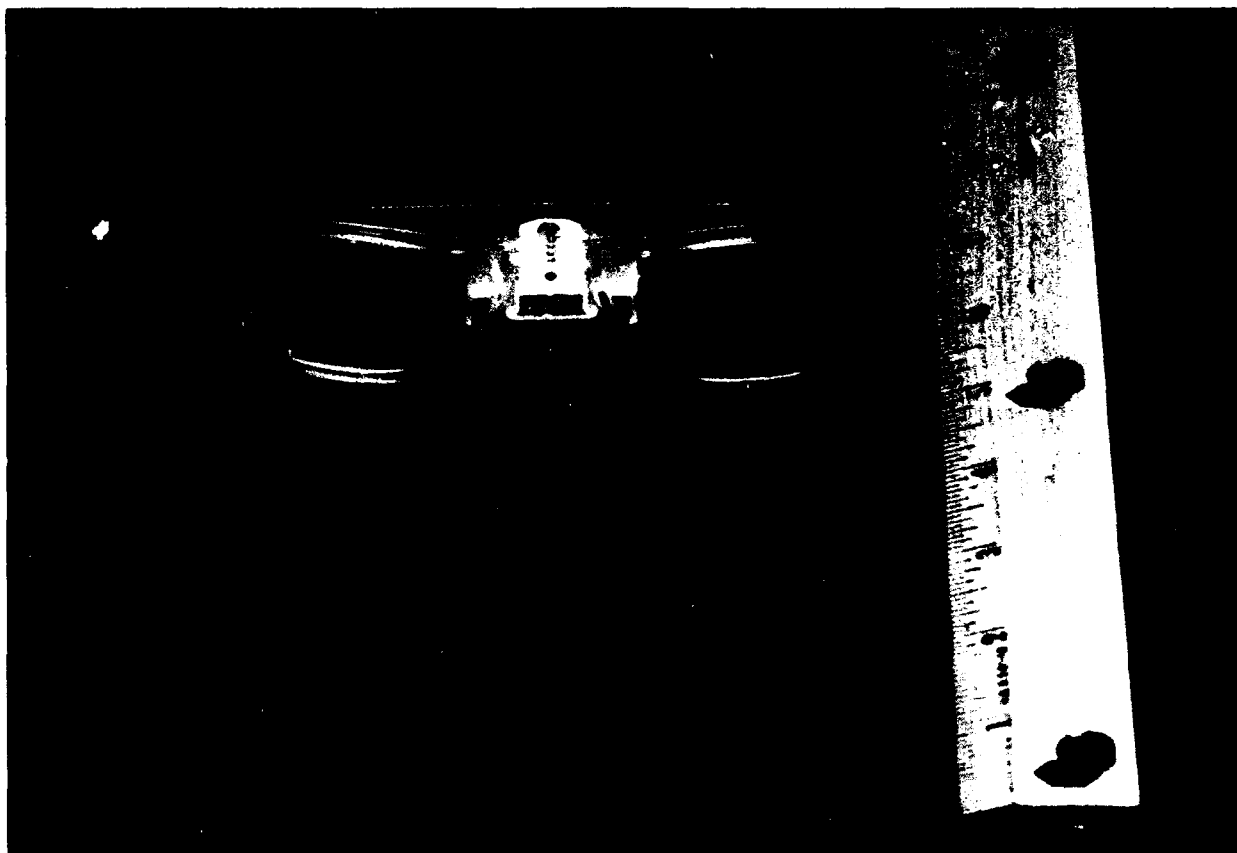


Figure 5. M40 preplanned product improvement visual correction with Velcro™ mount.

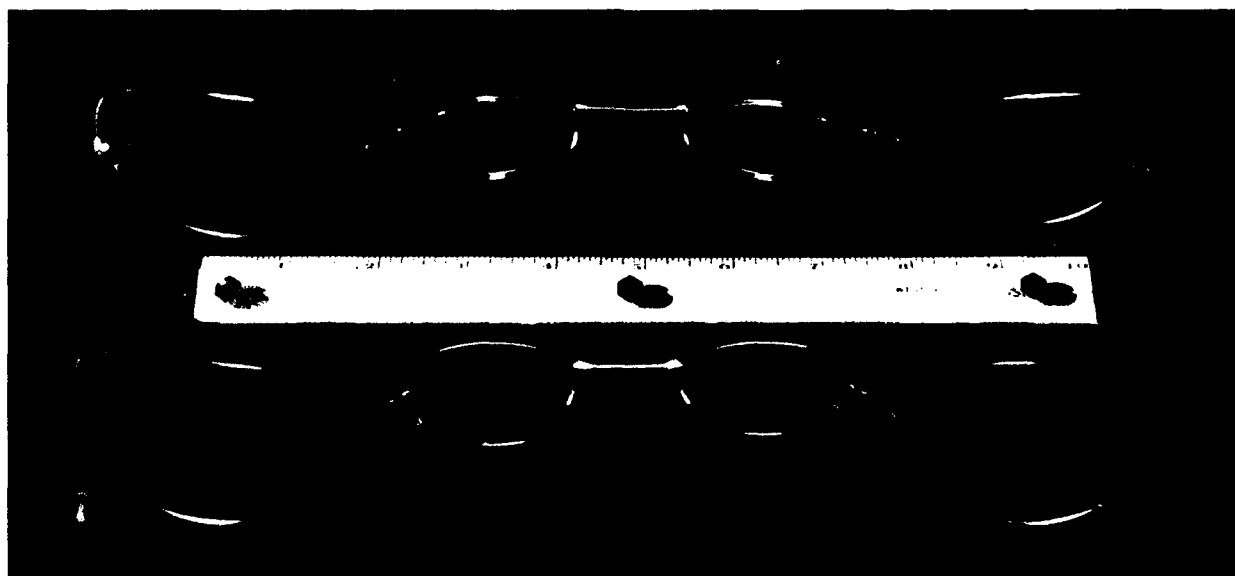


Figure 6. Two visual corrections used in M17 protective mask.

Table 1.  
Visual corrections tested.

Mask	Lens holder	Size (mm)	Mounting bracket
M17	Wire, obsolete	33	Integral eye well rings
M17	Wire, current	39	Integral eye well rings
M40	Wire, current	39	Integral eye well rings
M40	Plastic, developmental	45	Detachable eye well rings
M40	Plastic, developmental	45	Velcro™ bridge mount

vertex distance was measured in situ for one subject using a technique originally described by Kotulak, Little, and McCullough (1987). These measurements led to the development of a mathematical model which explains the results of the present experiment and makes predictions about how visual correction FOV varies with vertex distance in the M40.

Finally, the FOVs of the M17 and M40 masks without their visual corrections were measured. This was done to separate the field limiting effects of the mask apertures from those of the visual corrections. The mask with the smaller lens aperture, the M17, was found to have the larger FOV (Table 2). This finding is consistent with previous investigations (Rash and McLean, 1983; McLean and Rash, 1984; Rash and Crosley, 1985). To explain this effect, vertex distances of the mask lenses were measured in the manner described in the preceding paragraph for the M40 visual

Table 2.  
Size and curvature of mask lenses.

Mask	Horizontal diameter (mm)	Vertical diameter (mm)	Horizontal curvature (D)	Vertical curvature (D)
M17	84	69	+4.00	+1.00
M40	98	95	+8.00	0.00

corrections. Also, mask FOV data from the current study were compared to those of an earlier work (Rash and McLean, 1983) to determine whether FOV is relatively invariant across studies despite differences in subjects, mask fitting techniques, and FOV measuring methods.

### Methods

Subjects. The study included three subjects, who had interpupillary distances of 60, 66, and 69 mm, respectively. All subjects had visual acuities of at least 20/20 in each eye uncorrected at 33 cm, the test distance for the FOV measurements.

Mask fitting. Recent studies with the M43 protective mask have suggested that the accuracy of mask fit could influence FOV (Crosley and Kotulak, 1990; Crosley, Rash, and Levine, 1991). Therefore, in the present study the masks were sized from complete fitting sets by a technician who was qualified to fit the M17 and M40 by virtue of graduation from a formal training course. The technician selected the medium size of both masks for each subject.

Visual corrections. The visual corrections and the mounting brackets that were evaluated are each available in only one size. Table 1 describes each device. The values in the size column were computed by averaging the diameters of the aperture measured at 30° intervals.

FOV terminology. Previous M40 studies have specified FOV in a particular meridian as an angular measurement from a fixation point to a peripheral limit, i.e., the half field (Rash and McLean, 1983; McLean and Rash, 1984; Rash and Crosley, 1985). However, with the proliferation of night vision devices, an alternative method of FOV specification has gained wide acceptance (Wood, 1978; Neal, 1983; Brickner, 1989; Verona and Rash, 1989; Crowley, 1990). The latter method specifies FOV from peripheral limit to peripheral limit along a meridian which passes through fixation, i.e., the full field. This report uses the full field method of specifying FOV. Also in this report, the FOVs obtained from all test meridians are averaged, so that a single number is obtained which is used to represent the FOV of a given device. This simplifies comparisons between FOVs of competing design candidates.

If the FOV through a protective mask were measured separately for each eye while the contralateral eye is occluded, the two fields thus obtained would not entirely overlap when both eyes are open (Rash and McLean, 1983; McLean and Rash, 1984; Rash and Crosley, 1985). Instead, separate binocular and monocular regions of the total FOV could be identified. In this report, "binocular FOV" is defined as the region where, when both eyes are open, the two fields (measured as described above) overlap, and "monocular FOV" is defined as the region where they do not. "Total FOV" is defined as the sum of the binocular and monocular FOVs. Binocular fields were measured separately from monocular ones because a variety of visual functions are either unique to binocular vision (e.g., stereopsis) or behave differently under the two conditions (e.g., visual acuity). Several recent papers demonstrate this difference between binocular and monocular vision, e.g., Behar and Walsh (1988), low contrast visual acuity; Pardhan and Gilchrist (1990), contrast sensitivity; Blake, Zimba, and Williams (1985), motion perception; Heravian, Jenkins, and Douthwaite (1990), visually evoked responses; and Banton and Levi (1991), vernier acuity.

FOV apparatus. The FOV was measured with a dynamic arc perimeter which could project a spot of light along any meridian from 0 to 360° to any point along an arc within 100° of fixation (Figure 7). The test stimulus was a 10 mm diameter green circle located at 33 cm from the subject's eye. The target luminance was 2.5 cd/m<sup>2</sup>, while the background luminance was 0.2 cd/m<sup>2</sup>. The fixation point was a white cross which had a luminance of 3.5 cd/m<sup>2</sup>.

FOV measurement procedures. Red filters, which would not pass the green stimulus light, were placed in the lens holders of the mask's visual correction. The subject, with one eye occluded, was masked and seated with the chin portion of the mask

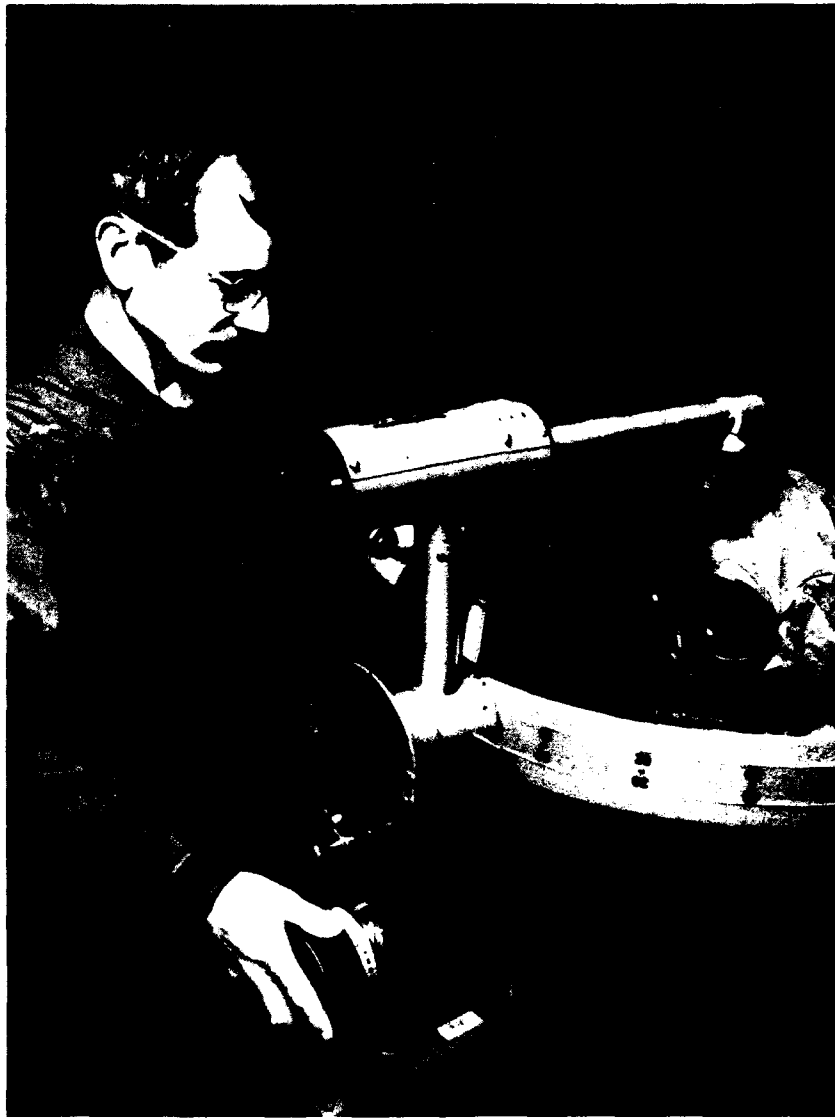


Figure 7. Field-of-view measurement apparatus.

in the chin rest of the perimeter. The subject was instructed to fixate the cross (which appeared red through the filter) and to tap the table once when the green stimulus light first appeared and to tap twice when it disappeared. The stimulus was moved from the periphery towards fixation until the subject's first signal. This point was recorded as the mask temporal FOV limit for the particular meridian under investigation. The stimulus was moved again in the same direction until the subject tapped twice. This point was recorded as the visual correction temporal FOV limit for the test meridian. The stimulus then was moved beyond fixation in the same direction. The subject also was instructed to tap once when the stimulus reappeared on the





Figure 8. Vertex distance measurement apparatus.

opposite side of fixation, and to tap twice when it disappeared a second time. The one-tap signal in this case represented the nasal limit of the visual correction FOV, while the two-tap signal represented the nasal limit of the mask FOV. This procedure was repeated at  $30^\circ$  intervals until all test meridians were measured for one eye, and then the other eye was measured in a similar fashion.

Vertex distance apparatus. The vertex distance was measured with a modified slitlamp biomicroscope (Figure 8) (Kotulak, Little, and McCullough, 1987). The principle modifications were: (1) replacement of the chin rest with a mask-compatible head rest, (2) mechanical and optical changes that allow the microscope to travel farther from the eye while maintaining a sharp focus, and (3) linkage of the microscope base to a digital electronic caliper to record the vertex distance measurements.

Vertex distance measurement procedures. A reference mark was placed on the anterior surface of the test lens (i.e., the mask lens or the visual correction lens) at a point directly

aligned with the center of the subject's pupil. The masked subject was seated with his head against the head rest. After the center of the subject's pupil was located through the microscope, the subject was instructed to close his eyes. The microscope then was focused on an anatomical landmark on the anterior surface of the subject's closed eyelid, and the caliper was zeroed. The landmark chosen was as close as possible to the center of his pupil. Then, the microscope was backed away until the reference mark on the test lens came into focus, at which time the caliper reading was recorded. This procedure was carried out 10 times for each eye, and the mean value (when corrected for eyelid and lens thickness), was taken as the vertex distance.

### Results

Note. For the sake of consistency, data from Rash and McLean (1983) (Figures 9-12) were converted to the format used in this report (see FOV terminology in the methods section above). The Rash and McLean study ( $n = 3$ ) is the only one available that reported data in sufficient detail to permit statistical comparisons with the data of the present investigation.

Total FOV through protective masks without visual corrections. Figure 9 presents data on total FOV through protective masks without visual corrections from the present study and from Rash and McLean for the M17 and the M40. In addition, Figure 9 contains total visual field (unmasked) data from Rash and McLean. The unmasked subjects had a mean visual field of  $160 \pm 6^\circ$ , which was reduced to  $137 \pm 6^\circ$  and  $125 \pm 3^\circ$  by the M17 and the M40 respectively according to Rash and McLean, and to  $135 \pm 10^\circ$  and  $127 \pm 9^\circ$  by the respective masks according to the present study.

Two types of statistical analyses were performed, one to determine whether the current study replicated the results of Rash and McLean, and the other to determine whether total FOVs were different between the two masks in general. The two-tailed T-test for independent samples indicated that the current study did in fact replicate the work of Rash and McLean, i.e., there was no statistical difference when the mean for each mask from one study was compared to the mean of the same mask from the other study (for the M17,  $df = 4$ ,  $T = 0.34$ , and  $p > 0.74$ ; for the M40,  $df = 4$ ,  $T = 0.39$ ,  $p > 0.71$ ). However, the question of whether total FOVs vary between the two masks is more complicated. The two-tailed T-test for paired samples indicated that total FOVs do indeed vary when comparing one mask to the other within the same investigation (for Rash and McLean,  $df = 2$ ,

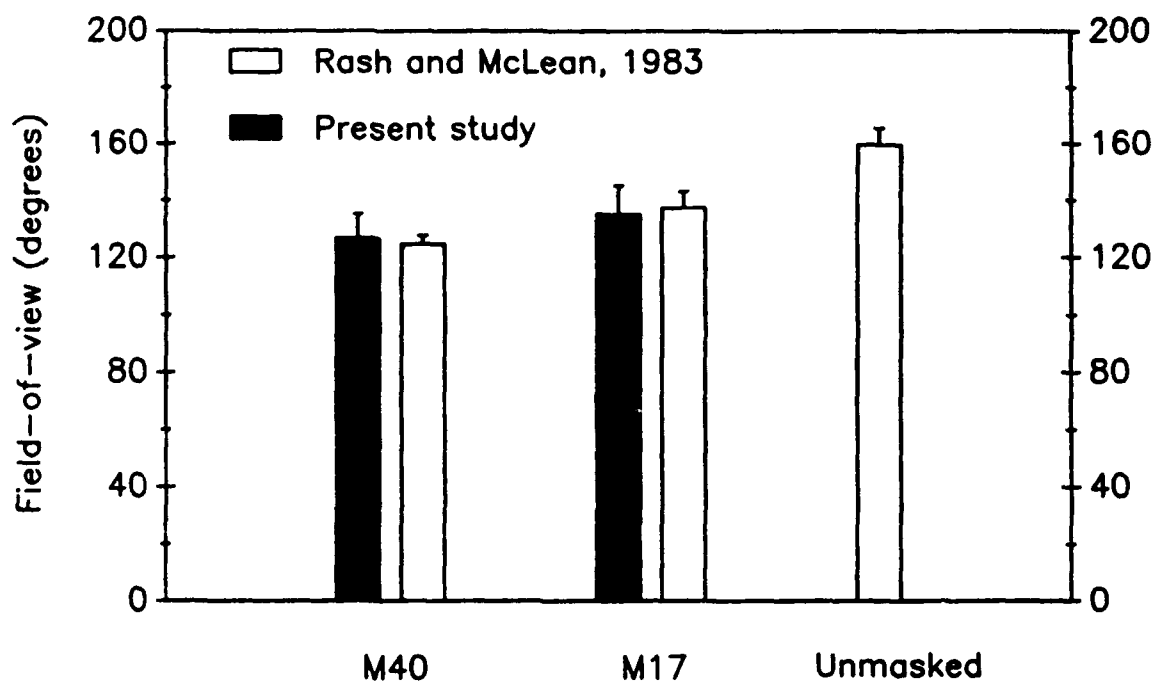


Figure 9. Total field-of-view wearing masks without visual corrections.

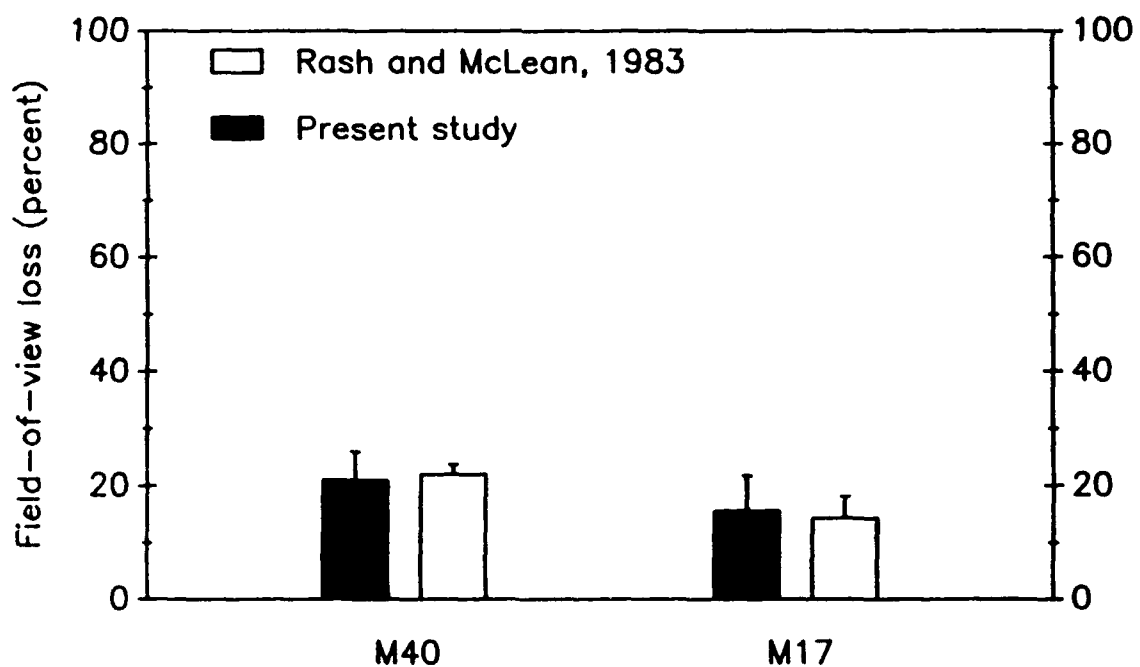


Figure 10. Loss to total field-of-view caused by wearing protective masks without visual corrections.

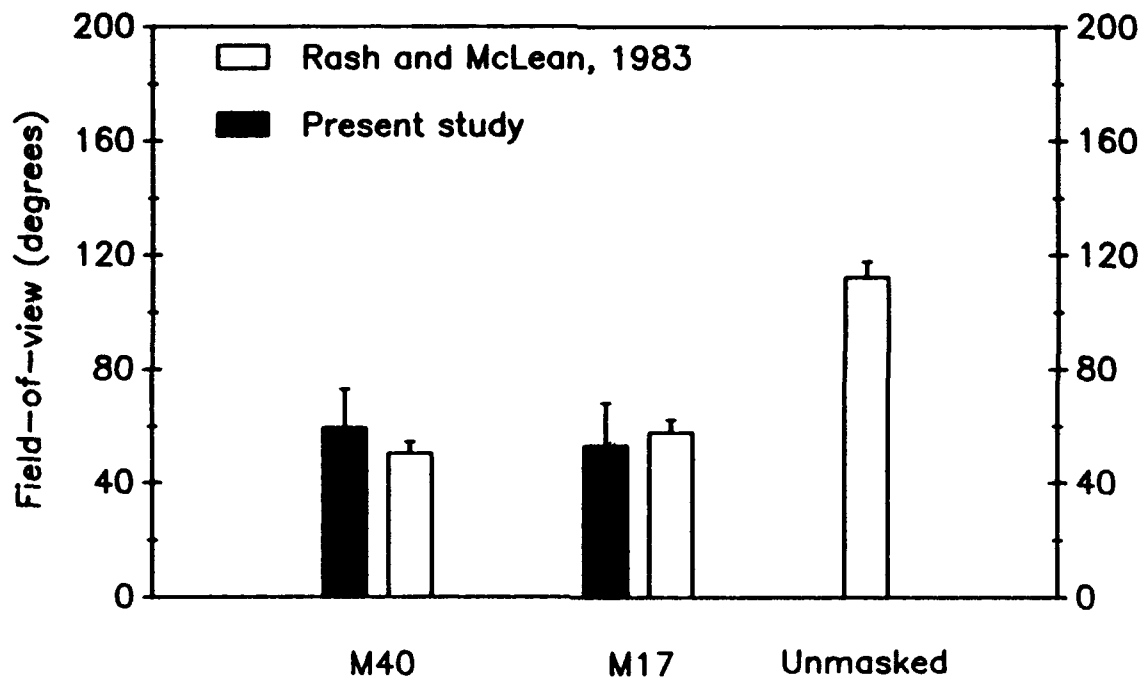


Figure 11. Binocular field-of-view wearing protective masks without visual corrections.

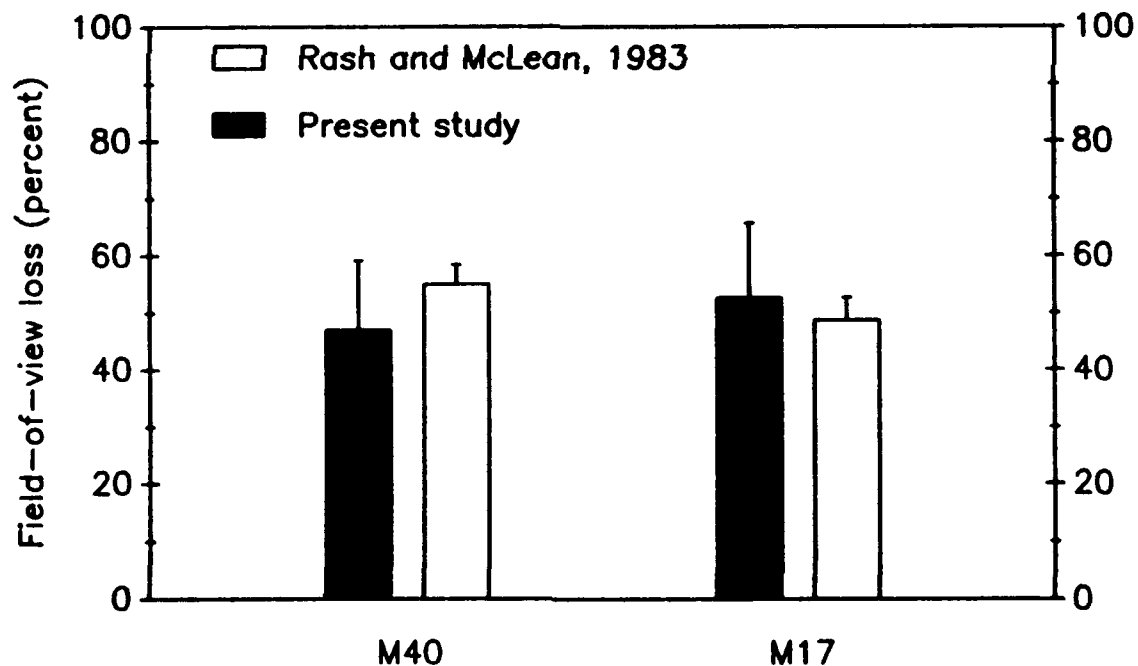


Figure 12. Loss to binocular field-of-view caused by wearing masks without visual corrections.

$T = 7.18$ ,  $p < 0.02$ ; for the current study,  $df = 2$ ,  $T = 5.74$ ,  $p < 0.03$ ). However, the opposite conclusion is reached if the two-tailed T-test for independent samples is used to compare one mask to the other between the two investigations (comparing M17 data of Rash and McLean to M40 data of the present study,  $df = 4$ ,  $T = 1.79$ ,  $p > 0.14$ ; comparing M17 data of the present study to M40 data of Rash and McLean,  $df = 4$ ,  $T = 1.70$ ,  $p > 0.16$ ).

Figure 10 is derived from the same data as Figure 9 and it expresses percent loss of total visual field attributable to the masks. These losses were 14 percent and 22 percent for the M17 and M40 respectively from Rash and McLean, and 16 percent and 21 percent for the respective masks from the present study.

Binocular FOV through protective masks without visual corrections. Figure 11 depicts the size of the binocular FOVs provided by the M17 and M40 masks without visual corrections from the present study and from Rash and McLean, as well as the binocular visual field (unmasked) data from Rash and McLean. The mean binocular visual field was  $112 \pm 6^\circ$ , which was reduced to  $58 \pm 5^\circ$  and  $50 \pm 4^\circ$  by the M17 and M40 respectively according to Rash and McLean, and to  $53 \pm 15^\circ$  and  $59 \pm 14^\circ$  by the respective masks according to the present study.

Statistical tests were performed (as in the case of total FOV above) with two distinct goals: to determine whether the current study replicated the results of Rash and McLean with respect to binocular FOVs, and to determine whether binocular FOVs differ between the two masks in general. As in the case of total FOV above, the two-tailed T-test for independent samples showed that the current study did indeed replicate the data of Rash and McLean, i.e., there was no statistical difference between the binocular FOV of either mask and that same mask in the other study, (for the M17,  $df = 4$ ,  $T = 0.51$ ,  $p > 0.63$ ; for the M40,  $df = 4$ ,  $T = 1.09$ ,  $p > 0.33$ ). Regarding the question of whether binocular FOVs vary between the two masks, the statistical procedures suggest that for the most part they do not. The two-tailed T-test for paired samples indicated that the binocular FOVs were different between the two masks for Rash and McLean ( $df = 2$ ,  $T = 22.00$ ,  $p < 0.003$ ) but no such difference was found for the current study ( $df = 2$ ,  $T = 0.46$ ,  $p > 0.69$ ). The two-tailed T-test for independent samples showed that the binocular FOVs did not vary between the two masks (comparing M17 data from Rash and McLean to M40 data from the present study,  $df = 4$ ,  $T = 0.20$ ,  $p > 0.85$ ; comparing M17 data from the present study to M40 data from Rash and McLean,  $df = 4$ ,  $T = 0.29$ ,  $p > 0.78$ ).

Figure 12 expresses the data of Figure 11 in terms of percent loss of binocular visual field caused by masks, which

were  $49 \pm 4$  percent and  $55 \pm 3$  percent according to Rash and McLean for the M17 and M40 respectively, and  $53 \pm 13$  percent and  $47 \pm 12$  percent for the respective masks according to the present study.

Total FOV through protective masks with visual corrections. Figure 13 illustrates the size of the total FOV through protective masks with visual corrections for the five devices listed in Table 1. The mean FOVs were:  $91 \pm 6^\circ$  and  $114 \pm 9^\circ$  for the M17 33 mm and 39 mm wire visual corrections respectively,  $93 \pm 8^\circ$  for the M40 39 mm wire visual correction, and  $92 \pm 10^\circ$  and  $96 \pm 16^\circ$  for the M40 Velcro<sup>TM</sup> and eye well visual corrections respectively. The means were not statistically different ( $df = 4/8$ ,  $F = 2.53$ ,  $p > 0.12$ ) by analysis of variance with repeated measures. Figure 14 expresses the same data as percent loss of visual field, which was  $43 \pm 4$  percent and  $29 \pm 6$  percent for the M17 33 mm and 39 mm wire devices respectively,  $42 \pm 5$  percent for the M40 39 mm wire device, and  $43 \pm 6$  percent and  $40 \pm 10$  percent for M40 Velcro<sup>TM</sup> and eye well devices respectively.

Binocular FOV through protective masks with visual corrections. Figure 15 gives the binocular FOV through protective masks with visual corrections for the five devices listed in Table 1. The mean FOVs were:  $53 \pm 15^\circ$  and  $56 \pm 4^\circ$  for the M17 33 mm and 39 mm wire visual corrections respectively,  $63 \pm 1^\circ$  for the M40 39 mm wire visual correction, and  $61 \pm 10^\circ$  and  $56 \pm 12^\circ$  for the M40 Velcro<sup>TM</sup> and eye well visual corrections respectively. An analysis of variance with repeated measures did not reveal a significant difference among the means ( $df = 4/8$ ,  $F = 0.45$ ,  $p > 0.76$ ). Figure 16 expresses the same data as percent loss of visual field, which was  $53 \pm 14$  percent and  $50 \pm 4$  percent for the M17 39 mm and 44 mm wire devices respectively,  $44 \pm 1$  percent for the M40 44 mm wire device, and  $45 \pm 9$  percent, and  $50 \pm 11$  percent for M40 Velcro<sup>TM</sup> and eye well devices respectively.

Mask lens size and vertex distance. Table 2 describes the size and shape of the facepiece assembly lenses of the M17 and M40 masks. The M40 lenses are larger than those of the M17. However, Figures 9 and 10 demonstrate that the mask with the smaller lenses, the M17, has the larger FOV. This can be true only if the M17 has the smaller vertex distance. Figure 17 gives vertex distance measurements for the M17 and M40 masks for a single subject. The mean vertex distances were  $25.8 \pm 2.3$  mm and  $28.5 \pm 1.3$  mm for the right and left lenses respectively of the M17, and  $34.7 \pm 1.2$  mm and  $36.2 \pm 1.2$  mm for the right and left lenses respectively of the M40. An analysis of variance with repeated measures found statistically significant main effects with mask type ( $df = 1/9$ ,  $F = 250.36$ , and  $p < 0.0001$ ) and with lens laterality (right versus left lens) ( $df = 1/9$ ,  $F = 45.86$ , and  $p < 0.0007$ ). The interaction between mask type and lens laterality was not significant ( $df = 1/9$ ,  $F = 1.56$ ,  $p > 0.24$ ).

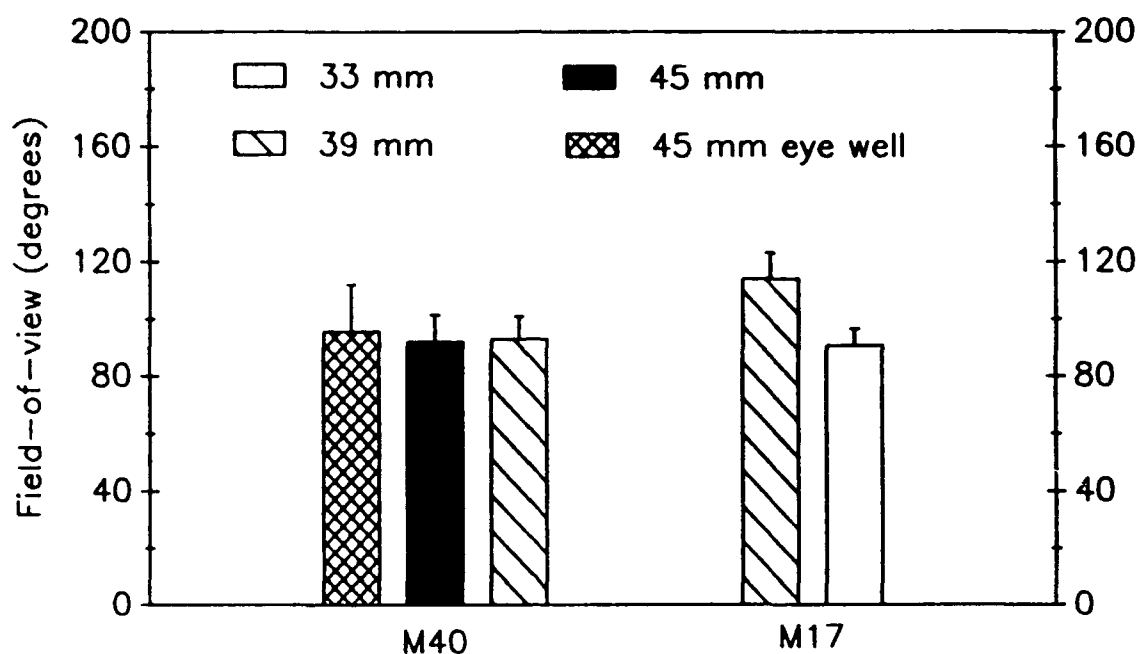


Figure 13. Total field-of-view wearing protective masks with visual corrections.

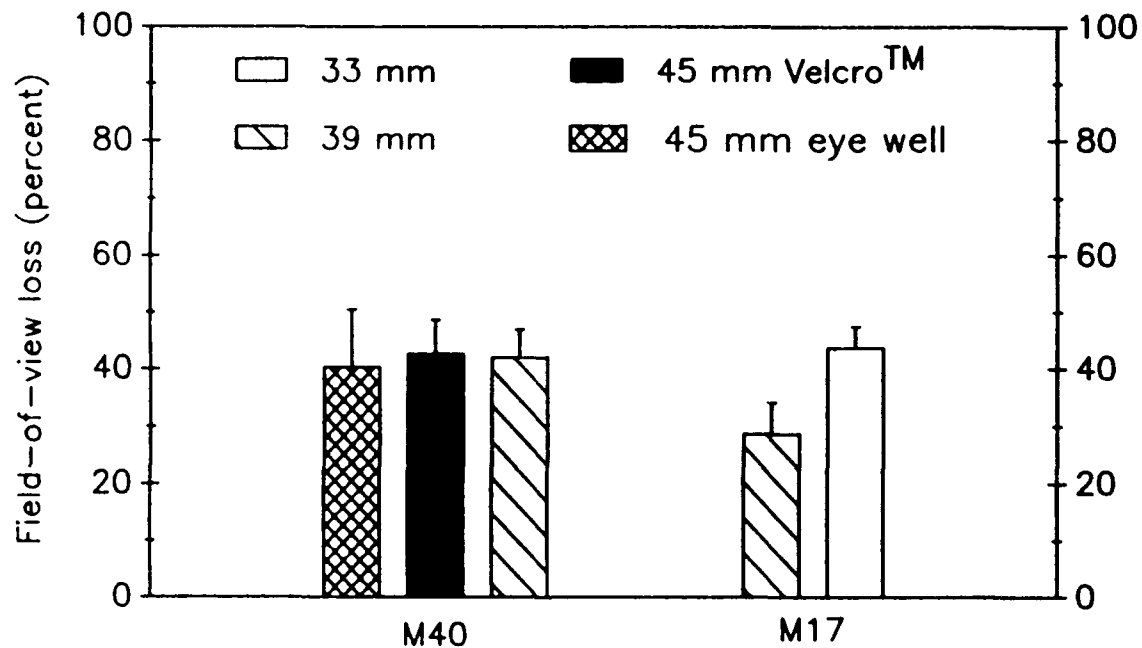


Figure 14. Loss to total field-of-view caused by wearing protective masks with visual corrections.

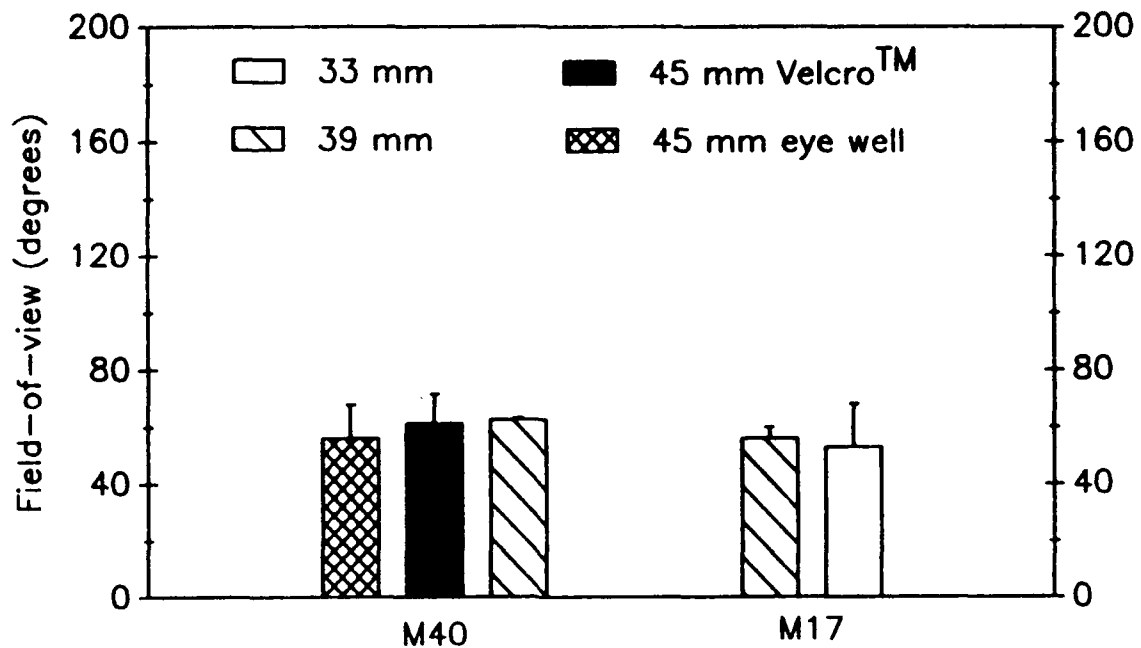


Figure 15. Binocular field-of-view wearing protective masks with visual corrections.

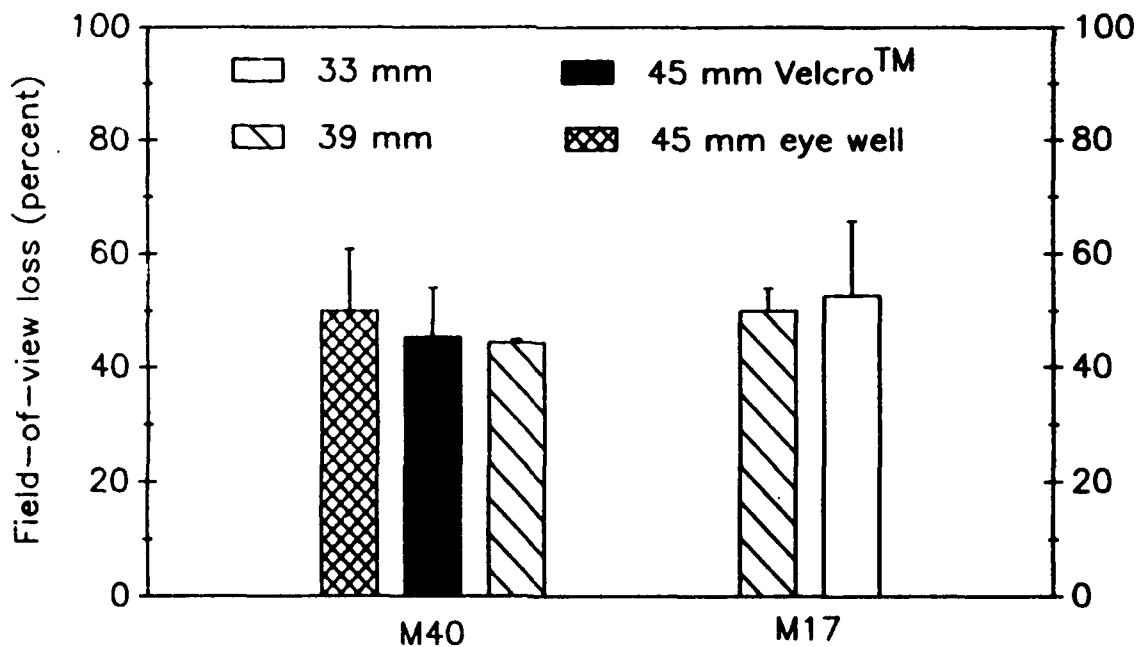


Figure 16. Loss to binocular field-of-view caused by wearing protective masks with visual corrections.



Visual correction vertex distance. Figure 18 shows how vertex distance varies among visual corrections for the same subject. The mean vertex distances were:  $9.4 \pm 1.4$  mm and  $8.7 \pm 1.3$  mm for the right and left lenses respectively for the current M17 correction,  $14.6 \pm 0.5$  mm and  $11.3 \pm 1.0$  mm of the right and left lenses respectively of the current M40 correction, and  $17.5 \pm 1.8$  mm and  $18.2 \pm 1.3$  mm for the right and left lenses of the M40 P<sup>3</sup>I correction. An analysis of variance with repeated measures revealed statistically significant main effects for the type of visual correction ( $df = 2/18$ ,  $F = 386.82$ , and  $p < 0.0001$ ) and for lens laterality ( $df = 1/9$ ,  $F = 16.39$ , and  $p < 0.008$ ). The interaction between type of correction and lens laterality was also statistically significant ( $df = 2/18$ ,  $F = 20.75$ ,  $p < 0.0001$ ). A contrast over a within factor analysis revealed each visual correction was statistically different from the other two, and that the interaction between type of correction and lens laterality was statistically significant except when the current M17 correction was paired with the M40 P<sup>3</sup>I correction (Table 3).

Figures 19 and 20 depict data from Davis and Kotulak (1986) on vertex distance for an earlier but similar version of the M40 P<sup>3</sup>I visual correction ( $n = 78$ ). Figure 19 is a histogram which gives the frequency distribution of vertex distance for all 78 subjects. Figure 20 displays average vertex distance separately for each eye and for each mask size. Davis and Kotulak found mean vertex distances of:  $25.7 \pm 3.8$  mm for size small masks ( $n = 16$ ),  $19.3 \pm 3.1$  mm for size medium masks ( $n = 49$ ), and  $23.6 \pm 4.6$  mm for size large masks ( $n = 13$ ). A one-way analysis of variance indicated that the differences between the three sample means were statistically significant ( $df = 2/75$ ,  $F = 23.89$ ,  $p < 0.000001$ ). Multiple comparison tests found no statistical difference only when the sized small sample was paired with the sized large one (Table 4).

The mean vertex distance (right and left lenses averaged) for the M40 P<sup>3</sup>I visual correction for the subject tested in the present experiment (Figure 18) is  $18.3 \pm 1.3$  mm. A two-tailed Z-test for comparing a sample mean to a population mean was performed to determine whether 18.3 mm was significantly different than the analogous value from Davis and Kotulak. The latter was taken to be 19.3 mm, the mean vertex distance for size medium M40s, because the subject from the present investigation wore a medium sized mask. The Z-test found no statistical difference between the two means ( $p > 0.25$ ).

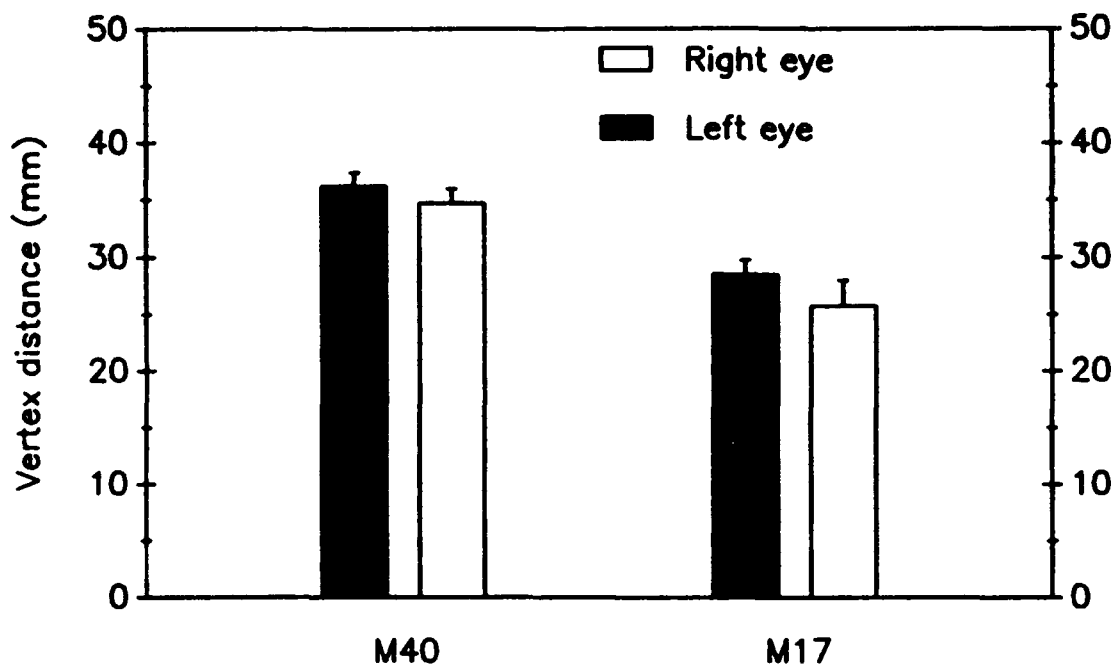


Figure 17. Effect of mask type on mask vertex distance.

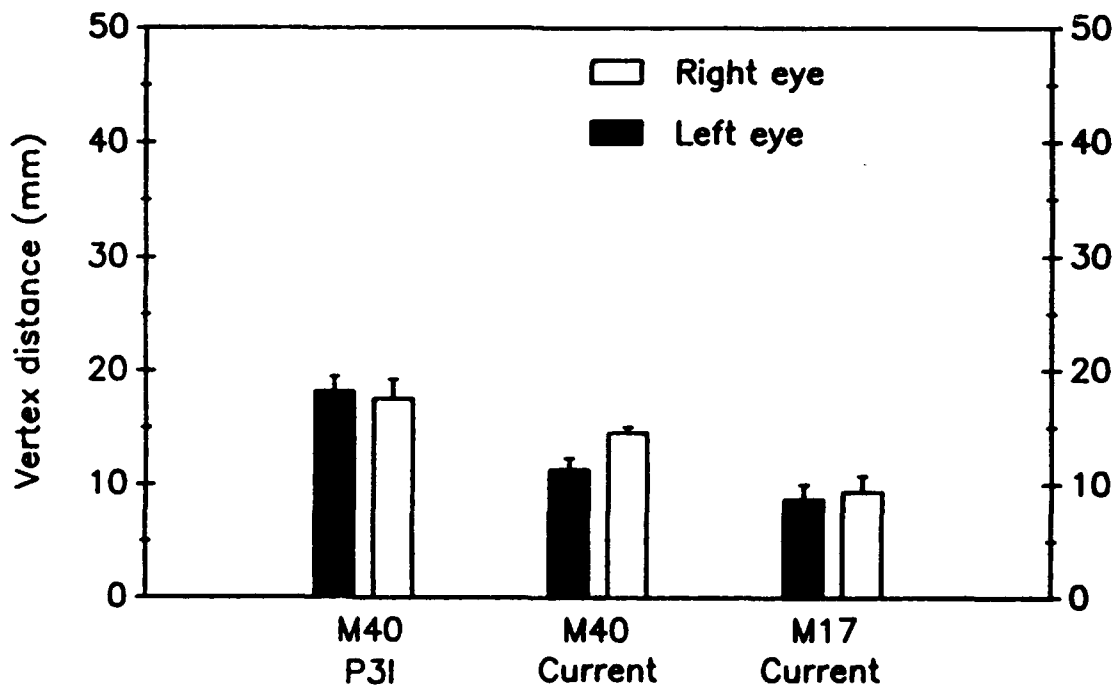


Figure 18. Effect of mask and visual correction type on visual correction vertex distance.

Table 3.

Contrast over a within factor.  
 Visual correction vertex distance  
 as a function of visual correction type.

Pairing	df	Main effect		Interaction	
		F	p	F	p
M17 current + M40 current	1/9	141.48	< 0.0001	35.34	< 0.0002
M17 current + M40 test	1/9	214.54	< 0.0001	2.72	> 0.13
M40 current + M40 test	1/9	220.25	< 0.0001	46.14	0.0001

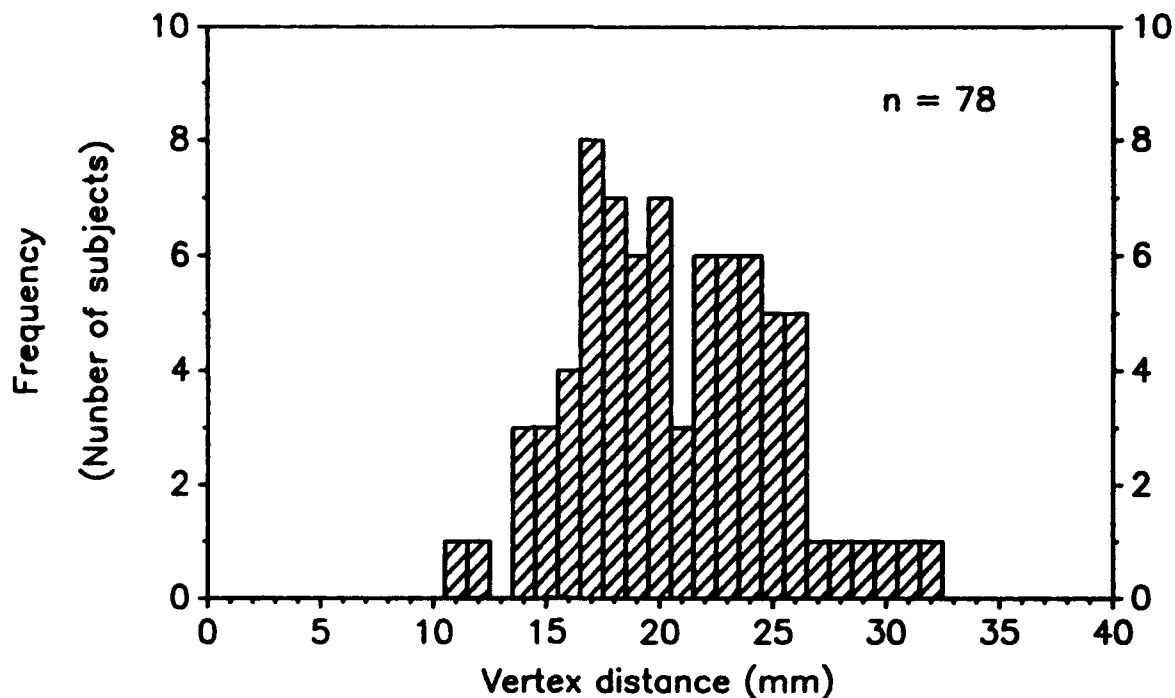


Figure 19. Vertex distance, M40 preplanned product improvement visual correction, all mask sizes combined.

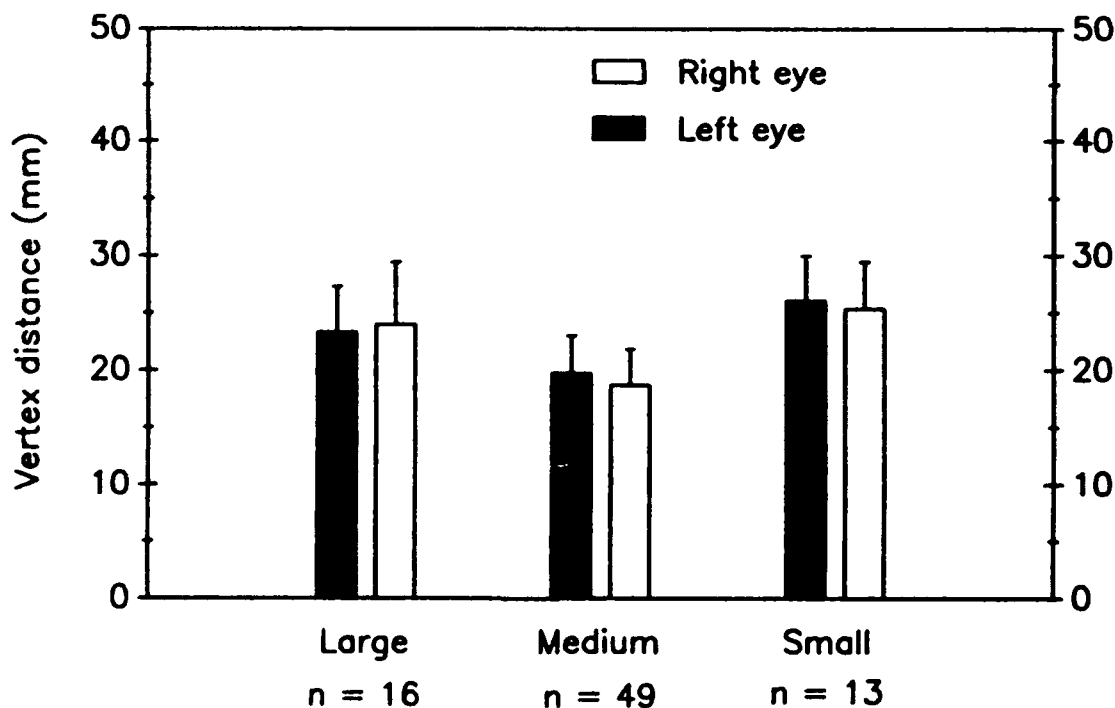


Figure 20. Effect of M40 mask size on preplanned product improvement visual correction vertex distance.

Table 4.

Multiple comparison tests.  
P<sup>3</sup>I vertex distance as function of M40 mask size.

Pairing	df	F	p
Small + Medium	1/63	47.26	< 0.000001
Small + Large	1/27	1.82	> 0.18
Medium + Large	1/60	16.69	< 0.0002

## Discussion

The M40 P<sup>3</sup>I visual correction, despite its larger lens apertures, fails to surpass the FOV of its predecessor, regardless of whether the eye well or Velcro™ mounting bracket is used (Table 1 and Figures 13-16). This is clearly related to a vertex distance differential between the P<sup>3</sup>I and current visual correction (Figure 18), which offsets the aperture size advantage of the P<sup>3</sup>I. A first order approximation of the relative contributions to FOV of visual correction lens aperture radius and vertex distance is given by Equation 1 below, in which  $\theta$  is the FOV,  $\alpha$  is the aperture radius, and  $\beta$  is the vertex distance.

$$\theta = 2\arctan(\alpha/\beta) \quad (1)$$

The predictions made by equation 1 are presented graphically in Figure 21. Equation 1 predicts a total FOV for the current M17 visual correction of 131°, while the measured one was 123°, a disagreement of 7 percent. For the current M40 visual correction, equation 1 predicts a total FOV of 113°, while the measured one was 101°, a disagreement of 12 percent. And for the P<sup>3</sup>I visual correction, both the predicted and measured total FOV were 101°.

Equation 1 ignores the effects of the mask lens apertures on visual correction FOV, which results in prediction errors of up to 12 percent. Equation 2 below is a second order approximation of visual correction FOV, which depends on the same two variables as equation 1. However, equation 2 contains a term which corrects for some of the field limiting effects of the M40 mask lens apertures.

$$\theta = 2\arctan(\alpha/\beta) - (-2.2\beta + 40.7) \quad (2)$$

Equations 1 and 2 are plotted in Figure 22, the former by filled circles and the latter by the open circles. Equation 2, while more accurate than equation (1), is more restrictive, i.e., it applies only to the M40 size medium mask and to vertex distances between 13 and 19 mm (because it was derived from limited empirical data). It is assumed that the functions merge for vertex distances greater than 19 mm, the point at which the field limiting effects of the visual correction become predominant over the field limiting effects of the mask.

The mathematical model represented in Figure 22 may be of value to developers in assessing the feasibility of improving FOV in the M40 P<sup>3</sup>I visual correction. It is theoretically possible to increase visual correction FOV by decreasing vertex distance, which could be accomplished by modifying the mounting bracket.

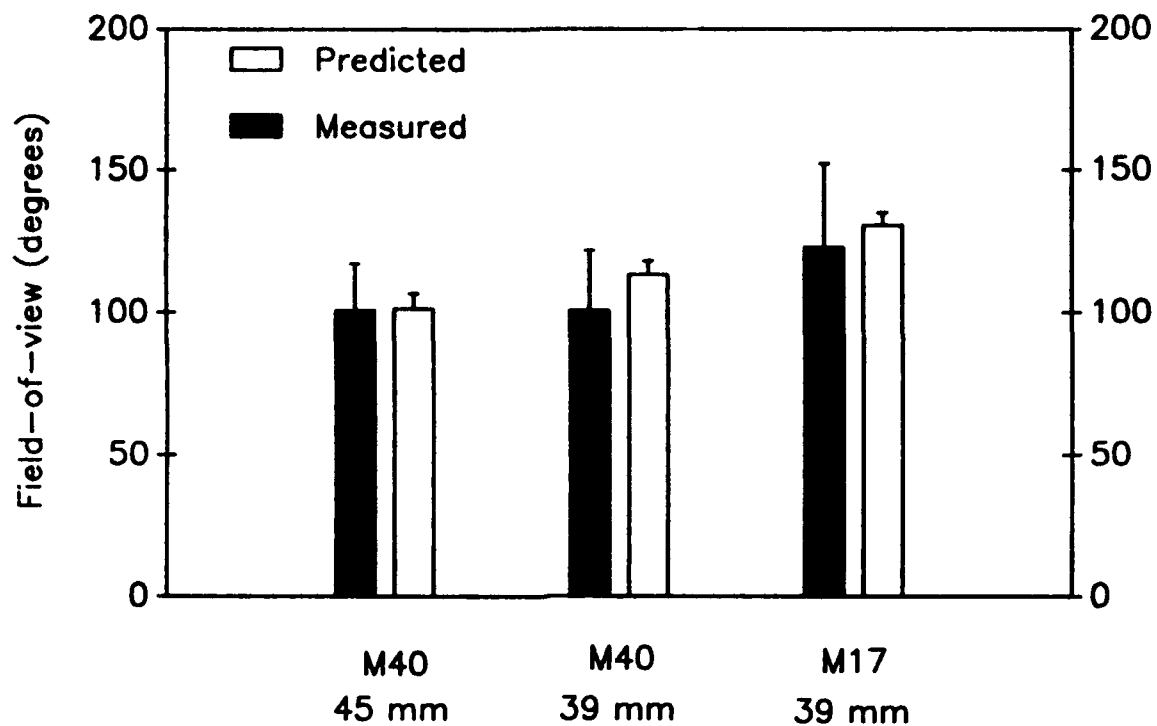


Figure 21. Predicted versus measured fields-of-view with visual corrections.

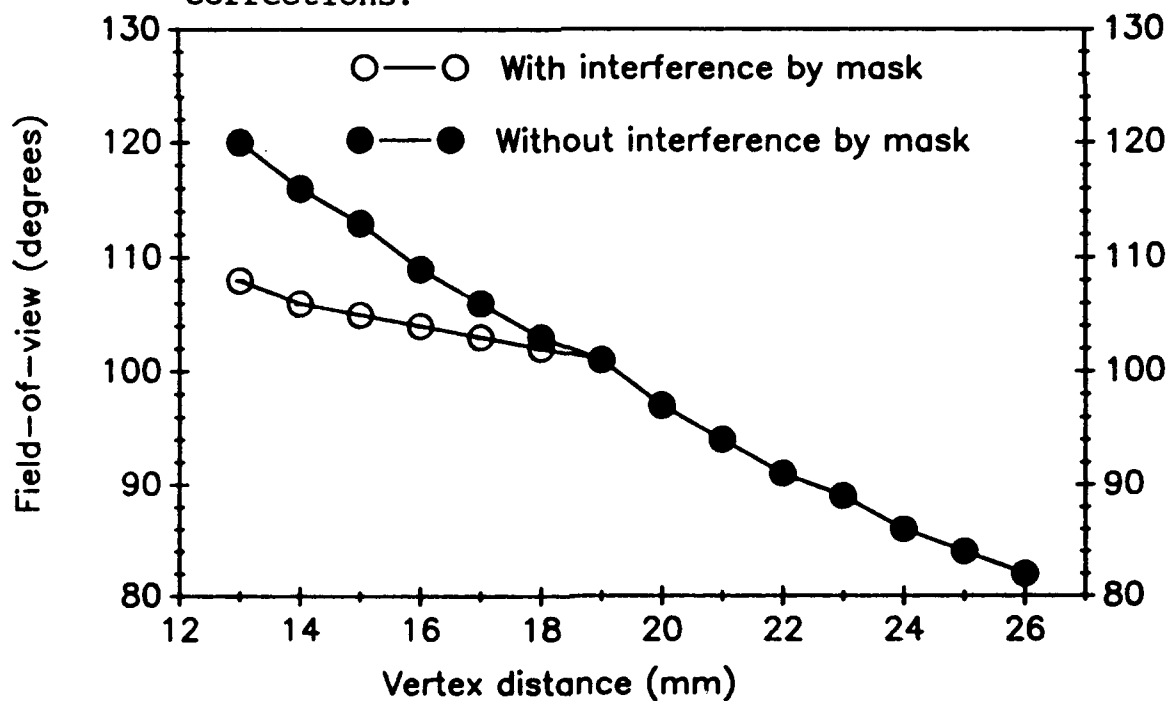


Figure 22. Theoretical field-of-view, M40 preplanned product improvement visual correction, with and without interference by mask.

However, for the size medium mask, which has a mean vertex distance of around 19 mm, the gain in FOV could be disappointing since the slope of the function which relates FOV to vertex distance is fairly flat when vertex distance is less than 20 mm (Figure 22). In addition, Figures 19 and 20 suggest that in a small percentage of individuals the eyelashes and forehead could come into physical contact with the visual correction if vertex distance were substantially reduced.

The absolute limit of the FOV of a visual correction is the FOV of the mask. For the M17, the 33 and 39 mm wire visual corrections provide 67 and 84 percent respectively of the mask FOV (in terms of average diameter). The analogous values for the M40 current, P<sup>3</sup>I Velcro™, and P<sup>3</sup>I eye well visual corrections are 73, 72, and 76 percent respectively. However, FOV loss induced by visual corrections is partially offset by a look-around capability. The soldier's visual acuity in the look-around area, the region between the visual correction and mask FOV limits in a particular meridian, is inversely related to the magnitude of his refractive error.

The FOV of the size small and large M40 masks was not directly determined in this study, because all of the test subjects required the size medium mask for proper fit. However, certain deductions are possible. The size small and large masks have mean visual correction vertex distances of around 26 and 24 mm respectively (Figure 20). From this, one could expect significant reductions in total FOV compared to the size medium mask. In addition, the visual correction vertex distance for the small and large mask sizes is of sufficient magnitude to influence the effective power of the prescription lenses. For example, prescription lenses with powers of -5.00, -4.00, and -3.00 diopter would lose -0.56, -0.36, and -0.21 diopter of power respectively at a vertex distance of 25 mm. Prescription changes of this magnitude could result in visual acuity losses of up to two lines on a letter chart (Smith, 1991).

The military significance of improving FOV beyond that already provided by the M40 P<sup>3</sup>I visual correction has not yet been demonstrated. Studies that have investigated the relationship between military task performance and FOV have generally found no association except when FOV falls below 60° (Wells, Venturino, and Osgood, 1988; Wells and Venturino, 1989; Osgood and Wells, 1991). This suggests that developers should not be discouraged by the failure of the M40 P<sup>3</sup>I visual correction to surpass the FOV of its predecessor. Factors such as comfort, cost, optical laboratory considerations, and visual acuity should probably take priority over FOV in this context.



This study, as well as previous ones of this type (Rash and McLean, 1983; McLean and Rash, 1984; Rash and Crosley, 1985), have used a sample size of 3. Although small samples are known to increase the likelihood of Type II statistical error (Dowdy and Wearden, 1983), we do not feel that Type II error played a significant role in our analysis. This is because our conclusions were based more on operational considerations than on statistical inference. To illustrate this, consider our main conclusion: the FOVs of the P<sup>3</sup>I visual corrections, which were 92 and 96° for the Velcro™ and eye well devices respectively, are not significantly larger than the FOV of the current M40 visual correction, which was 93°. Even if, by substantially increasing the sample size, 96° were found to be statistically greater than 93°, no operational significance could be attached to this finding.

### Conclusions

1. The proposed M40 P<sup>3</sup>I visual correction results in a FOV that is no larger than that of its predecessor, regardless of which mounting system is used.
2. There is no advantage of one M40 P<sup>3</sup>I mounting system over the other with respect to FOV.
3. M40 P<sup>3</sup>I visual correction vertex distance in the size small and large M40 masks is excessive. Potentially, this can be remedied by modifying the mounting bracket.

## References

- Banton, T., and Levi, D. M. 1991. Binocular summation in vernier acuity. Journal of the optical society of America. 8: 673-680.
- Behar, I., and Walsh, D. J. 1988. Binocular summation for resolution and contrast sensitivity test charts. Paper presented at the annual meeting of the Aerospace Medical Association, 12 May, New Orleans, LA.
- Blake, R., Zimba, L., and Williams, D. 1985. Visual motion, binocular correspondence, and binocular rivalry. Biological cybernetics. 52: 391-397.
- Brickner, M. S. 1989. Helicopter flights with night vision goggles - human factors aspects. Moffett Field, CA: NASA Ames Research Center. NASA Technical Memorandum No. 101039.
- Crosley, J. K., and Kotulak, J. C. 1990. Visual evaluation of M43 protective mask frontserts. Fort Rucker, AL: U.S. Army Aeromedical Research Laboratory. USAARL LR 91-3-2-3.
- Crosley, J. K., Rash, C. E., and Levine, R. R. 1991. Visual and field-of-view evaluation of the M43 protective mask with prescription eyepieces. Fort Rucker, AL: U.S. Army Aeromedical Research Laboratory. USAARL Report No. 91-13.
- Crowley, J. S. 1990. Human factors aspects of helicopter accidents with night vision goggles in use. Fort Rucker, AL: U.S. Army Safety Center. Unnumbered report.
- Davis, J. D., and Kotulak, J. C. 1986. Measurements of faceform angle, pantoscopic angle, and vertex distance of the preplanned product improvement optical insert in two design candidates of the M40 protective mask. Aberdeen Proving Ground, MD: U.S. Army Environmental Hygiene Agency. Unpublished report.
- Dowdy, S., and Wearden, S. 1983. Statistics for research. New York: John Wiley and Sons.
- Heravian, J. S., Jenkins, T. C. A., and Douthwaite, W. A. 1990. Binocular summation in visually evoked responses and visual acuity. Ophthalmic and physiological optics. 10: 257-261.
- Kotulak, J. C. 1987. Occupational vision evaluation of feasibility study of interchangeable lens carrier. Aberdeen Proving Ground, MD: U.S. Army Environmental Hygiene Agency. Unnumbered letter report.

- Kotulak, J. C., Little, M. E., and McCullough, W. W. 1987. Determination and physiological assessment of the spatial parameters of testbed mask lenses, February-April 1987. Aberdeen Proving Ground, MD: U.S. Army Environmental Hygiene Agency. Occupational Vision Study No. 65-32-0049-87.
- McLean, W. E., and Rash, C. E. 1984. Visual and optical evaluations of the engineering design test prototypes of the XM40 CB mask. Fort Rucker, AL: U.S. Army Aeromedical Research Laboratory. USAARL LR-85-4-2-3.
- Neal, T. 1983. ANVIS - now a system designed for aviators! Aviation digest. 29: 12-17.
- Osgood, R. K., and Wells, M. J. 1991. The effect of field of view size on performance of a simulated air to ground night attack. Paper presented at AGARD symposium on helmet mounted displays and night vision goggles, 2 May, Pensacola, FL.
- Pardhan, S., and Gilchrist, J. 1990. The effect of monocular defocus on binocular contrast sensitivity. Ophthalmic and physiological optics. 10: 33-36.
- Rash, C. E., and Crosley, J. K. 1985. Visual and optical evaluations of the XM40 CB mask in support of Development Test II. Fort Rucker, AL: U.S. Army Aeromedical Research Laboratory. USAARL LR-85-8-2-5.
- Rash, C. E., and McLean, W. E. 1983. Visual and optical evaluations of the XM40 protective mask. Fort Rucker, AL: U.S. Army Aeromedical Laboratory. USAARL LR-83-9-2-6.
- Schapero, M., Cline, D., and Hofstetter, H. W., eds. 1968. Dictionary of visual science. 2nd ed. Radnor, PA: Chilton Book Co.
- Smith, G. 1991. Relation between spherical refractive error and visual acuity. Optometry and vision science. 68: 591-598.
- Verona, R. W., and Rash, C. E. 1989. Human factors and safety considerations of night vision systems flight. Fort Rucker, AL: U.S. Army Aeromedical Research Laboratory. USAARL Report No. 89-12.
- Wells, M. J., and Venturino, M. 1989. The effect of increasing task complexity on the field-of-view requirements for a visually coupled system. In Proceedings of the Human Factors Society 33rd annual meeting, volume 1, 91-95. Human Factors Society. Santa Monica, CA.

Wells, M. J., Venturino, M., and Osgood, R. K. 1988. Using target replacement performance to measure spatial awareness in a helmet mounted simulator. In Proceedings of the Human Factors Society 32nd annual meeting, volume 2, 1429-1433. Human Factors Society. Santa Monica, CA.

Wood, W. C. 1978. Human factors aspects of the AN/PVS-5 night vision goggle. Aviation digest. 24: 32-35.

Appendix A

Extract from tasking document

(e) Vision Correction Mounting System (VCMS).

Subtest	CRDEC	HEL	USAARL	Ft Knox (IOTE)
Human Factors	-	X	-	X
Field of View	-	X	X	X
Visual Field	-	-	X	-
Quality of Vision Correction	-	X	-	X
RAM & Durability	X	X	-	X
Training	-	X	-	X
Environmental Storage	X	-	-	-
Compatibility	X	X	-	X
Wear and Carry	-	X	-	X
Adverse Environment/Rough Handling	X	-	-	-

1 USAARL. 3 M40 P3I masks with 5 each of the prototype mounts: Field of view.

2 HEL.

- M16 rifle firing: 12 soldiers with 36 targets per VCMS per soldier.

- Obstacle course: 12 soldiers with one VCMS on worn mask, another VCMS on a carried mask through an obstacle course. 2 trials per VCMS.

- Donning: 12 soldiers with 2 trials per VCMS per soldier.

- Field of view: 12 soldiers on M1 tank and M19 binoculars.

(4) Limitations.

c. Production Qualification Test (PQT). Separate PQTs will be performed for each improvement to ensure that the P3I elements meet JSOR requirements and are representative of the prototype masks during PPQT and IOTE.

D. PART IV--OT&E OUTLINE

1. Operational Test and Evaluation (OT&E) Overview. The TEXCOM will assist in preparing for, and conduct of, operational testing of product improvements. Testing will be conducted at the location which will afford the most complete operational and economical testing for each item to be tested.

2. Critical Operational Issues. The following issues and their respective criterion were extracted from the Draft Critical Operational Issues and Criteria (COIC) For The M40-Series Chemical-Biological (CB) Protective Mask Preplanned Product Improvement (P3I), September 14 1990.

## Appendix B

### Technical description current and P<sup>3</sup>I M40 visual corrections

The current M40 visual correction (Figure 2), which is worn inside the mask, is a one-piece assembly with no user-detachable parts. Each prescription lens is held in place by a metal rim, which is affixed to a wire mounting ring by means of a rod and sleeve mechanism. The rod extends from the lens holder and it fits into the sleeve's proximal end. The sleeve is pierced orthogonally at its distal end by the mounting ring. Both the rod and the mounting ring are free to pivot within the sleeve. The mounting rings insert into their respective facepiece lens wells. The lens holders are connected to each other by a spring coil. This arrangement allows the visual correction to fit within the physical confines of the mask despite a wide range of facial anthropometric variability among mask users. Unfortunately, this arrangement also permits the lenses to move independently of one another and to adopt spatial orientations inconsistent with optimum optical performance (Kotulak, 1987).

A proposed new visual correction for the M40 has been developed by the U.S. Army Medical Materiel Development Activity and the U.S. Army Chemical Research, Development, and Engineering Center. This new device, which is referred to as a "preplanned product improvement" (P<sup>3</sup>I), also is worn inside the mask but differs from its predecessor in several respects, such as lens size and shape, frame composition, and method of attachment. Unlike the current visual correction, which is a one-piece assembly, the P<sup>3</sup>I version has two parts: the interchangeable lens carrier and the mounting bracket.

The interchangeable lens carrier (Figure 3) is already in use with ballistic-laser protective spectacles (hence the name "interchangeable"). It is similar to a spectacle frame without temples (side pieces), and it consists of two plastic lens holders which accept standard aviator style lenses. The lens holders are joined together by a spring-loaded hinge, which permits movement in only the posterior direction. The anterior edges of the hinge are tapered for insertion into the dovetail tracks of the mounting bracket.

Two prototypes currently exist for the mounting bracket (Figures 4 and 5). Both designs are plastic and secure the interchangeable lens carrier to the bridge of the facepiece-lens assembly of the mask. One concept (Figure 4) anchors the bracket to the mask eye wells in the manner of the M40 mounting rings, with the important difference that both mounting rings attach to a common point rather than to each lens holder independently.

The second concept (Figure 5) attaches the bracket to the mask by means of Velcro™. Both prototypes provide the interchangeable lens carrier with a single point of attachment to the mask, which greatly reduces the chance of malpositioning of the prescription lenses.



## Initial distribution

Commander, U.S. Army Natick Research,  
Development and Evaluation Center  
ATTN: STRNC-MIL (Documents  
Librarian)  
Natick, MA 01760-5040

Col. Otto Schramm Filho  
c/o Brazilian Army Commission  
Office-CEBW  
4632 Wisconsin Avenue NW  
Washington, DC 20016

Commander/Director  
U.S. Army Combat Surveillance  
and Target Acquisition Lab  
ATTN: DELCS-D  
Fort Monmouth, NJ 07703-5304

Commander  
10th Medical Laboratory  
ATTN: Audiologist  
APO New York 09180

Naval Air Development Center  
Technical Information Division  
Technical Support Detachment  
Warminster, PA 18974

Commanding Officer, Naval Medical  
Research and Development Command  
National Naval Medical Center  
Bethesda, MD 20814-5044

Deputy Director, Defense Research  
and Engineering  
ATTN: Military Assistant  
for Medical and Life Sciences  
Washington, DC 20301-3080

Commander, U.S. Army Research  
Institute of Environmental Medicine  
Natick, MA 01760

U.S. Army Avionics Research  
and Development Activity  
ATTN: SAVAA-P-TP  
Fort Monmouth, NJ 07703-5401

U.S. Army Communications-Electronics  
Command  
ATTN: AMSEL-RD-ESA-D  
Fort Monmouth, NJ 07703

Library  
Naval Submarine Medical Research Lab  
Box 900, Naval Sub Base  
Groton, CT 06349-5900

Commander  
Man-Machine Integration System  
Code 602  
Naval Air Development Center  
Warminster, PA 18974

Commander  
Naval Air Development Center  
ATTN: Code 602-B (Mr. Brindle)  
Warminster, PA 18974

Commanding Officer  
Harry G. Armstrong Aerospace  
Medical Research Laboratory  
Wright-Patterson  
Air Force Base, OH 45433

Director  
Army Audiology and Speech Center  
Walter Reed Army Medical Center  
Washington, DC 20307-5001

Commander, U.S. Army Institute  
of Dental Research  
ATTN: Jean A. Setterstrom, Ph. D.  
Walter Reed Army Medical Center  
Washington, DC 20307-5300

Naval Air Systems Command  
Technical Air Library 950D  
Room 278, Jefferson Plaza II  
Department of the Navy  
Washington, DC 20361

Director, U.S. Army Human  
Engineering Laboratory  
ATTN: Technical Library  
Aberdeen Proving Ground, MD 21005

Commander, U.S. Army Test  
and Evaluation Command  
ATTN: AMSTE-AD-H  
Aberdeen Proving Ground, MD 21005

Director  
U.S. Army Ballistic  
Research Laboratory  
ATTN: DRXBR-OD-ST Tech Reports  
Aberdeen Proving Ground, MD 21005

Commander  
U.S. Army Medical Research  
Institute of Chemical Defense  
ATTN: SGRD-UV-AO  
Aberdeen Proving Ground,  
MD 21010-5425

Commander, U.S. Army Medical  
Research and Development Command  
ATTN: SGRD-RMS (Ms. Madigan)  
Fort Detrick, Frederick, MD 21702-5012

Director  
Walter Reed Army Institute of Research  
Washington, DC 20307-5100

HQ DA (DASG-PSP-O)  
5109 Leesburg Pike  
Falls Church, VA 22041-3258

Harry Diamond Laboratories  
ATTN: Technical Information Branch  
2800 Powder Mill Road  
Adelphi, MD 20783-1197

U.S. Army Materiel Systems  
Analysis Agency  
ATTN: AMXSU-PA (Reports Processing)  
Aberdeen Proving Ground  
MD 21005-5071

U.S. Army Ordnance Center  
and School Library  
Simpson Hall, Building 3071  
Aberdeen Proving Ground, MD 21005

U.S. Army Environmental  
Hygiene Agency  
Building E2100  
Aberdeen Proving Ground, MD 21010

Technical Library Chemical Research  
and Development Center  
Aberdeen Proving Ground, MD  
21010-5423

Commander  
U.S. Army Medical Research  
Institute of Infectious Disease  
SGRD-UIZ-C  
Fort Detrick, Frederick, MD 21702

Director, Biological  
Sciences Division  
Office of Naval Research  
600 North Quincy Street  
Arlington, VA 22217

Commander  
U.S. Army Materiel Command  
ATTN: AMCDE-XS  
5001 Eisenhower Avenue  
Alexandria, VA 22333

Commandant  
U.S. Army Aviation  
Logistics School ATTN: ATSQ-TDN  
Fort Eustis, VA 23604

Headquarters (ATMD)  
U.S. Army Training  
and Doctrine Command  
ATTN: ATBO-M  
Fort Monroe, VA 23651

Structures Laboratory Library  
USARTL-AVSCOM  
NASA Langley Research Center  
Mail Stop 266  
Hampton, VA 23665

Naval Aerospace Medical  
Institute Library  
Building 1953, Code 03L  
Pensacola, FL 32508-5600

Command Surgeon  
HQ USCENTCOM (CCSG)  
U.S. Central Command  
MacDill Air Force Base FL 33608

Air University Library  
(AUL/LSE)  
Maxwell Air Force Base, AL 36112

U.S. Air Force Institute  
of Technology (AFIT/LDEE)  
Building 640, Area B  
Wright-Patterson  
Air Force Base, OH 45433

Henry L. Taylor  
Director, Institute of Aviation  
University of Illinois-Willard Airport  
Savoy, IL 61874

Chief, Nation Guard Bureau  
ATTN: NGB-ARS (COL Urbauer)  
Room 410, Park Center 4  
4501 Ford Avenue  
Alexandria, VA 22302-1451

Commander  
U.S. Army Aviation Systems Command  
ATTN: SGRD-UAX-AL (MAJ Gillette)  
4300 Goodfellow Blvd., Building 105  
St. Louis, MO 63120

U.S. Army Aviation Systems Command  
Library and Information Center Branch  
ATTN: AMSAV-DIL  
4300 Goodfellow Boulevard  
St. Louis, MO 63120

Federal Aviation Administration  
Civil Aeromedical Institute  
Library AAM-400A  
P.O. Box 25082  
Oklahoma City, OK 73125

Commander  
U.S. Army Academy  
of Health Sciences  
ATTN: Library  
Fort Sam Houston, TX 78234

Commander  
U.S. Army Institute of Surgical Research  
ATTN: SGRD-USM (Jan Duke)  
Fort Sam Houston, TX 78234-6200

AAMRL/HEX  
Wright-Patterson  
Air Force Base, OH 45433

John A. Dellinger,  
Southwest Research Institute  
P. O. Box 28510  
San Antonio, TX 78284

Product Manager  
Aviation Life Support Equipment  
ATTN: AMCPM-ALSE  
4300 Goodfellow Boulevard  
St. Louis, MO 63120-1798

Commander  
U.S. Army Aviation  
Systems Command  
ATTN: AMSAV-ED  
4300 Goodfellow Boulevard  
St. Louis, MO 63120

Commanding Officer  
Naval Biodynamics Laboratory  
P.O. Box 24907  
New Orleans, LA 70189-0407

Assistant Commandant  
U.S. Army Field Artillery School  
ATTN: Morris Swott Technical Library  
Fort Sill, OK 73503-0312

Commander  
U.S. Army Health Services Command  
ATTN: HSOP-SO  
Fort Sam Houston, TX 78234-6000

HQ USAF/SGPT  
Bolling Air Force Base, DC 20332-6188

U.S. Army Dugway Proving Ground  
Technical Library, Building 5330  
Dugway, UT 84022

U.S. Army Yuma Proving Ground  
Technical Library  
Yuma, AZ 85364

AFFTC Technical Library  
6510 TW/TSTL  
Edwards Air Force Base,  
CA 93523-5000

Commander  
Code 3431  
Naval Weapons Center  
China Lake, CA 93555

Aeromechanics Laboratory  
U.S. Army Research and Technical Labs  
Ames Research Center, M/S 215-1  
Moffett Field, CA 94035

Sixth U.S. Army  
ATTN: SMA  
Presidio of San Francisco, CA 94129

Commander  
U.S. Army Aeromedical Center  
Fort Rucker, AL 36362

U.S. Air Force School  
of Aerospace Medicine  
Strughold Aeromedical Library Technical  
Reports Section (TSKD)  
Brooks Air Force Base, TX 78235-5301

Dr. Diane Damos  
Department of Human Factors  
ISSM, USC  
Los Angeles, CA 90089-0021

U.S. Army White Sands  
Missile Range  
ATTN: STEWS-IM-ST  
White Sands Missile Range, NM 88002

U.S. Army Aviation Engineering  
Flight Activity  
ATTN: SAVTE-M (Tech Lib) Stop 217  
Edwards Air Force Base, CA 93523-5000

Ms. Sandra G. Hart  
Ames Research Center  
MS 262-3  
Moffett Field, CA 94035

Commander, Letterman Army Institute  
of Research  
ATTN: Medical Research Library  
Presidio of San Francisco, CA 94129

Commander  
U.S. Army Medical Materiel  
Development Activity  
Fort Detrick, Frederick, MD 21702-5009

Commander  
U.S. Army Aviation Center  
Directorate of Combat Developments  
Building 507  
Fort Rucker, AL 36362

U. S. Army Research Institute  
Aviation R&D Activity  
ATTN: PERI-IR  
Fort Rucker, AL 36362

Commander  
U.S. Army Safety Center  
Fort Rucker, AL 36362

U.S. Army Aircraft Development  
Test Activity  
ATTN: STEBG-MP-P  
Cairns Army Air Field  
Fort Rucker, AL 36362

Commander U.S. Army Medical Research  
and Development Command  
ATTN: SGRD-PLC (COL Sedge)  
Fort Detrick, Frederick, MD 21702

MAJ John Wilson  
TRADOC Aviation LO  
Embassy of the United States  
APO New York 09777

Netherlands Army Liaison Office  
Building 602  
Fort Rucker, AL 36362

British Army Liaison Office  
Building 602  
Fort Rucker, AL 36362

Italian Army Liaison Office  
Building 602  
Fort Rucker, AL 36362

Directorate of Training Development  
Building 502  
Fort Rucker, AL 36362

Chief  
USAHEL/USAAVNC Field Office  
P. O. Box 716  
Fort Rucker, AL 36362-5349

Commander U.S. Army Aviation Center  
and Fort Rucker  
ATTN: ATZQ-CG  
Fort Rucker, AL 36362

Commander/President  
TEXCOM Aviation Board  
Cairns Army Air Field  
Fort Rucker, AL 36362

MAJ Terry Newman  
Canadian Army Liaison Office  
Building 602  
Fort Rucker, AL 36362

German Army Liaison Office  
Building 602  
Fort Rucker, AL 36362

LTC Patrice Cottebrune  
French Army Liaison Office  
USAAVNC (Building 602)  
Fort Rucker, AL 36362-5021

Australian Army Liaison Office  
Building 602  
Fort Rucker, AL 36362

Dr. Garrison Rapmund  
6 Burning Tree Court  
Bethesda, MD 20817

Commandant Royal Air Force  
Institute of Aviation Medicine  
Farnborough Hampshire GU14 6SZ UK

Commander  
U.S. Army Biomedical Research  
and Development Laboratory  
ATTN: SGRD-UBZ-I  
Fort Detrick, Frederick, MD 21702

Defense Technical Information Center  
Cameron Station  
Alexandria, VA 22313

Commander, U.S. Army Foreign Science  
and Technology Center  
AIFRTA (Davis)  
220 7th Street, NE  
Charlottesville, VA 22901-5396

Director,  
Applied Technology Laboratory  
USARTL-AVSCOM  
ATTN: Library, Building 401  
Fort Eustis, VA 23604

U.S. Air Force Armament  
Development and Test Center  
Eglin Air Force Base, FL 32542

Commander, U.S. Army Missile  
Command  
Redstone Scientific Information Center  
ATTN: AMSMI-RD-CS-R  
/ILL Documents  
Redstone Arsenal, AL 35898

Dr. H. Dix Christensen  
Bio-Medical Science Building, Room 753  
Post Office Box 26901  
Oklahoma City, OK 73190

U.S. Army Research and Technology  
Laboratories (AVSCOM)  
Propulsion Laboratory MS 302-2  
NASA Lewis Research Center  
Cleveland, OH 44135

Dr. Christine Schlichting  
Behavioral Sciences Department  
Box 900, NAVUBASE NLON  
Groton, CT 06349-5900

COL Eugene S. Channing, O.D.  
Brooke Army Medical Center  
ATTN: HSHS-EAH-O  
Fort Sam Houston, TX 78234-6200

LTC Gaylord Lindsey (5)  
USAMRDC Liaison at Academy  
of Health Sciences  
ATTN: HSHA-ZAC-F  
Fort Sam Houston, TX 78234

Aviation Medicine Clinic  
TMC #22, SAAF  
Fort Bragg, NC 28305

Dr. A. Kornfield, President  
Biosearch Company  
3016 Revere Road  
Drexel Hill, PA 29026

NVEOD  
AMSEL-RD-ASID  
(Attn: Trang Bui)  
Fort Belvoir, VA 22060